# Conformational Space and Dynamic Stereochemistry of Overcrowded Homomerous Bistricyclic Aromatic Enes − A Theoretical Study

**P. Ulrich Biedermann,[a,b] John J. Stezowski,[c] and Israel Agranat*[a]**

*In Memoriam Dr. Yitzhak Tapuhi* [d]

**Keywords:** Conformational analysis / Enantiomerizations / Isomerizations / Semiempirical calculations / Strained molecules

The conformational spaces and dynamic stereochemistry of representative overcrowded homomerous bistricyclic aromatic enes (**1**, X = Y) are investigated, applying the semiempirical PM3 method. The experimental energy barriers for *E,Z* isomerizations, enantiomerizations, and conformational inversions of **1** and related compounds, derived from DNMR and other kinetic studies, are reviewed. This study focuses on the analysis of the minima, transition states, and dynamic mechanisms of the conformational isomerizations of bifluorenylidene (**2**), dixanthylene (**3**), dithioxanthylene (**9**), and bi-5*H*-dibenzo[*a,d*]cyclohepten-5-ylidene (**11**). The four representative bistricyclic enes differ in the sizes of their central rings and in their bridging groups. The mechanisms of the interconversions of the twisted, *anti*-folded, and *syn*-folded conformations and of thermal *E,Z* isomerizations (topomerizations), enantiomerizations, and conformational inversions (including combinations) are elucidated. The calculated energy barriers for *E,Z* topomerizations of **2**, **3**, **9**, and **11** are 25.3, 16.4, 24.3, and 39.3 kcal/mol, respectively. The corresponding barriers for enantiomerizations or conformational inversions are 4.9, 15.9, 24.3, and 37.6 kcal/mol, respectively. In most cases, the agreement with experimentally determined values is within 1–3 kcal/mol. New mechanisms are proposed for the *E,Z* isomerizations and conformational inversions of *anti*-folded **3**, **9**, and **11**, involving low-symmetry folded/twisted transition states and the respective *syn*-folded intermediates.

## 1. Introduction

The bistricyclic aromatic enes[1,2] (**1**) have fascinated chemists since bifluorenylidene (**2**) was synthesized in 1875,[3] dixanthylene (**3**) was synthesized in 1895,[4] and thermochromism and piezochromism were revealed in bianthrone (**4**).[5,6] They can be classified into *homomerous* bistricyclic enes (**1**, X = Y) and *heteromerous* bistricyclic enes (**1**, X ≠ Y).[7] They may be viewed as bridged tetraarylethylenes or as tetrabenzofulvalenes. These systems are attractive substrates for the study of the ground state conformations and dynamic stereochemistry of overcrowded polycyclic aromatic enes (PAEs).[1,2,8,9] The topic of bistricyclic enes has been reviewed previously.[1,2,9,10,11]

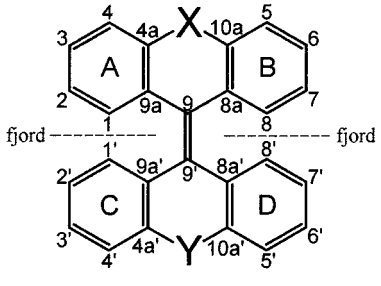


**1**

Thermochromic and photochromic bistricyclic enes are candidates for potential molecular switches.[12−16] Bifluorenylidene (**2**) and bi-4*H*-cyclopenta[*def*]phenanthren-4-ylidene (**5**),[17] with their central five-membered rings, are fullerene fragments, and potential starting materials for the preparation of buckyballs.[18−27] Lucigenin (**6**), a dicationic salt derived from *N,N′*-dimethylbiacridan (**1**, X,Y: $NCH_3$), was considered the most powerful of all synthetic chemiluminescent substances.[28,29] Bianthrone (**4**) is found in plants,[30]

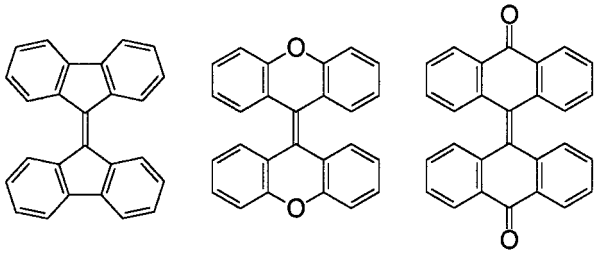

**2** **3** **4**

[a] Department of Organic Chemistry, The Hebrew University of Jerusalem,
Jerusalem 91904, Israel
Fax: (internat.) + 972-2/651-1907
E-mail: isria@vms.huji.ac.il
[b] Institut für Organische Chemie, Universität Stuttgart,
Pfaffenwaldring 55, 70569 Stuttgart, Germany
[c] Department of Chemistry, University of Nebraska-Lincoln,
Lincoln, NE 68588-0304, USA
[d] Dedicated to the memory of the Late Dr. Yitzhak Tapuhi (1948−1982), a brilliant scientist and a pioneer in the dynamic stereochemistry of overcrowded bistricyclic aromatic enes.

**MICROREVIEWS:** This feature introduces the readers to the authors' research through a concise overview of the selected topic. Reference to important work from others in the field is included.

  1434−193X/01/0101−0015 $ 17.50+.50/0 

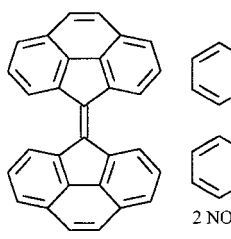


**5** **6** **7**

and its derivatives are topologically related to the natural product hypericin (**7**), abundant in St. John's wort (hypericum perforatum, German: Johanneskraut), an important remedy for depression,[31,32] and an antiretroviral agent with potential anti-AIDS capabilities.[33,34]

The thermochromism in solution of bianthrones, dixanthylenes, and several other bistricyclic enes has been shown to result from a thermal equilibrium between two distinct and interconvertible conformers (**A** ⇄ **B**), where **A** is the ground state, *anti*-folded, yellow conformer, and **B** is the thermochromic, green or blue, twisted conformer.[11,35−40] Conformers of type **A** and **B** have also been detected (along with other conformers) in studies of the photochromic and piezochromic phenomena exhibited by bianthrones, dixanthylenes, and some other bistricyclic enes. It is generally accepted that the thermochromic **B** conformer and the photochromic **B** conformer are identical. *Syn*-folded conformers of bistricyclic enes with central six-membered rings have been reported as metastable conformations − the photochromic **E** form − in the cases of, for example, 10,10′-dimethylbiacridan (**8**) (**1**, X,Y: $NCH_3$), dithioxanthylene (**9**) (**1**, X,Y: S), and the methylene-bridged bistricyclic ene **10** (**1**, X,Y: $CH_2$).[39−42] Piezochromism of bistricyclic enes has so far gained only little attention.[40,43] Values of $\Delta H°$ have been determined for the thermochromic equilibrium **A** ⇄ **B** in bianthrones and dixanthylene.[38,44−46] No direct correlation was found between $\Delta H°$ values and possible steric interactions in the fjord regions.[38] The thermal decay of the colored **B** species of 2,2′-bis(trifluoromethyl)bianthrone has been studied by laser flash photolysis ($\Delta H^{‡}_{B\rightarrow A}$). The relationship between the thermochromic process and the fast thermal *E*,*Z* isomerization found in the bianthrone series indicated that both thermal phenomena have a common highest transition state.[38] Thermochromism has also been found in the solid state.[47,48] The **A** → **B** transformation can be triggered not only by heating, photoexcitation, and pressure, but also by electrochemical redox cycles.[2,49−59] The important role of conformational equilibrium and kinetics in electrode reactions in the bianthrone series has been noted.[58]

This microreview is focused mainly on the analysis of the minima and transition states of the conformational spaces

*P. Ulrich Biedermann was born in 1962 in Sindelfingen, Germany. He received his Diplom in Chemistry in 1990 from the University of Stuttgart, Germany, started his Ph. D. research at the Institut für Organische Chemie there under the supervision of Professor John J. Stezowski and followed an invitation from Professor Israel Agranat to work on his Ph. D. thesis in Jerusalem. He was a Minerva Fellow 1991-1993 and received a Kurzstipendium of the Deutscher Akademischer Austauschdienst (DAAD) in 1995 for studies in Lincoln, Nebraska. He worked 1995/1996 as a Research Assistant in the research group "Chirality of Drugs and Chiral Recognition: New Challenges" at The Institute for Advanced Studies at The Hebrew University of Jerusalem. His Ph. D. research includes synthetic, NMR, X-ray crystallographic, and theoretical studies of overcrowded bistricyclic aromatic enes.*

*John J. Stezowski is Professor of Chemistry at the University of Nebraska − Lincoln. He was born in Chicago, Illinois in 1942, received his B. Sc. degree in Chemistry from Case Institute of Technology in 1964. Graduate studies in association with Professor Harry A. Eick were completed with a Ph. D. in Chemistry at Michigan State University awarded in1969; while at MSU Prof. Stezowski received the DuPont Teaching Award. Late in 1968, he joined the Chemistry Department at Cornell University in Ithaca, New York as a Postdoctoral Research Associate (National Institutes of Health Fellowship) in association with J. Lynn Hoard and Robert E. Hughes. In 1972, Professor Stezowski moved to the Institut für Organische Chemie der Universität Stuttgart; his Habilitation was completed in 1981; in 1986, he was appointed as a Universitätsprofessor for Structural Chemistry at the Universität Stuttgart. In 1991, Professor Stezowski joined the Chemistry Department at the University of Nebraska in Lincoln, Nebraska. His research interests are focused primarily on structural studies of complex organic molecules, especially supramolecular inclusion complexes with β-cyclodextrin hosts.*

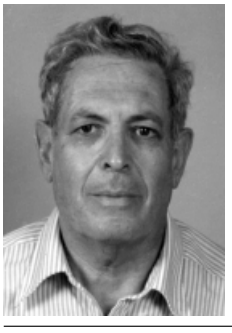

*Israel Agranat is Professor Ordinarius of Organic Chemistry at The Hebrew University of Jerusalem (HUJ) (since 1978), Visiting Professor at Imperial College School of Medicine (1999-2002), and an Editor-in-Chief of "Enantiomer: a Journal of Stereochemistry" (since 2000). Israel Agranat was born in Haifa, Israel in 1935. He studied Chemistry and Physics at HUJ and received his M. Sc. in Chemistry (1961) and Ph.D. in Organic Chemistry (1967) under the supervision of the Late Professor Ernst David Bergmann (1903-1975). Israel Agranat was a Research Fellow both in Chemistry at Harvard University with Professor William E. Doering (1968-1969) and in Medicinal Chemistry at Northeastern University with Professor Albert H. Soloway (1969-1970). Since 1970, he has been teaching at HUJ. Israel Agranat served as Chair, Vice-Chair, and Secretary of the European Federation for Medicinal Chemistry (1988-1996). He was a Fellow of the Institute of Advanced Studies at HUJ (1995-1996), where he directed a research group on "Chirality of Drugs and Chiral Recognition: New Challenges". In 1997, he held the Jawaharlal Nehru Chair at the University of Hyderabad, India. Agranat's "first love" in Chemistry was Aromaticity, which he considers a theoretical notion. He was among the inventors of triafulvenes and triapentafulvalenes and of the "Agranat Cation". Israel Agranat's research interests include chiral drugs, with special emphasis on chiral switches and intellectual property, novel aromatics, large PAHs, reversible Friedel−Crafts acylations, mechanisms of chiral distinction, cinchona alkaloids, the guanidine entity in medicinal chemistry, fluorine chemistry. The present Microreview illustrates Agranat's conviction of the importance of the interplay between theory and experiment.*

for a set of representative homomerous bistricyclic aromatic enes, with the emphasis on the mechanisms of conformational isomerizations. This set was selected from the 45 bistricyclic enes previously reviewed,[2] for a detailed study of conformational behavior. This study includes a search for possible conformations of lower symmetry, and for transition states involved in conformational isomerizations, including enantiomerizations and/or inversions of the conformations. The mechanisms of the dynamic stereochemistry are elucidated. The homomerous bistricyclic enes studied are bifluorenylidene (**2**) (**1**, X,Y: −), dixanthylene (**3**) (**1**, X,Y: O), dithioxanthylene (**9**) (**1**, X,Y: S), and bi-5*H*-dibenzo[*a*,*d*]cyclohepten-5-ylidene (**11**) (**1**, X,Y: CH=CH). The four homomerous enes differ in the size of their central rings and in their bridging groups. The conformational energies of the twisted conformations, relative to the respective *anti*-folded conformations, have been shown to vary over a wide range of values: −4.6 kcal/mol to +50.5 kcal/mol.[2] The semiempirical method PM3 was employed.[60] For bistricyclic enes, PM3 geometries are close to those found by X-ray crystallography.[2]

*Intramolecular Overcrowding* is a steric effect shown by aromatic structures in which certain (intramolecular) distances between nonbonded atoms are smaller than the sum of the van der Waals radii of the atoms involved.[61,62] The bistricyclic aromatic enes **1** are overcrowded in the fjord regions. This intramolecular overcrowding requires out-of-plane deformations to alleviate prohibitively close contacts of nonbonded atoms in the fjord regions on both sides of the central double bond ($C^9=C^{9'}$) resulting from the sterically demanding tricyclic moieties.

A variety of conformations has been identified in the homomerous bistricyclic enes series.[1] The nonplanarity of bifluorenylidene was inferred as early as 1935, from the dipole moment of 2,2′-difluorobifluorenylidene.[63] Red bifluorenylidene (**2**), with central five-membered rings, adopts a twisted conformation.[7,35,64−67] Yellow dixanthylene (**3**)[7,47,48,68] and bianthrone (**4**),[7,69−71] with central six-membered rings, are *anti*-folded with boat-shaped central rings. Colorless 5,5′-bi-5*H*-dibenzo[*a*,*d*]cycloheptenylidene (**11**), with central seven-membered rings, can adopt both an *anti*-folded and a *syn*-folded conformation.[72−76] $^1$H NMR spectroscopy has been used to distinguish between twisted, *anti*-folded, and *syn*-folded conformations of **1** in solution.[2,77]

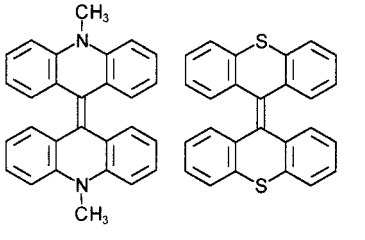


**8** **9**

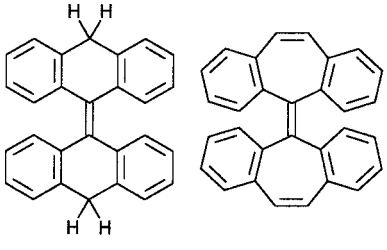


**10** **11**

### 1.1 Nonplanarity in Overcrowded Bistricyclic Enes

Two principal modes of out-of-plane deformations of enes are considered: twisting around the double bond and out-of-plane bending.[10,78] In **1**, the bending is brought about by folding about the $C^9\cdots X$ and $C^{9'}\cdots Y$ axes of the tricyclic moieties at both ends of the central ene, resulting in boat conformations in the central rings.

The pure twist ω of the central ethylene group is defined as the average of the signed torsion angles $\tau(C^{9a}-C^9-C^{9'}-C^{9a'})$ and $\tau(C^{8a}-C^9-C^{9'}-C^{8a'})$:[1]

$$\omega = 1/2\,[\tau(C^{9a}-C^9-C^{9'}-C^{9a'}) + \tau(C^{8a}-C^9-C^{9'}-C^{8a'})] \quad (1)$$

In addition to the twist in the double bond, the carbon atoms $C^9$ and $C^{9'}$ of the ethylene group may be pyramidalized.[79−85] This out-of-plane deformation results in a change in the pure $sp^2$ hybridization (towards $sp^3$),[80,81,83] and improves the π-overlap across the adjacent formal single bonds.[85] Pyramidalization of $C^9$ and $C^{9'}$ may lead to *syn* and to *anti* pyramidalization, as shown in Figure 1.

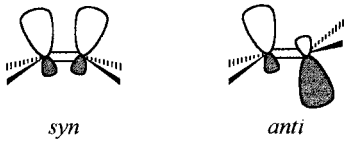

*syn* *anti*

Figure 1. Hybridization in *syn*- and *anti*-pyramidalized double bonds

Various measures for pyramidalization have been used in the literature.[80−84] In this study, the pyramidalization angle $\chi(C^9)$ − defined as the improper torsion angle $\tau(C^{9a}-C^9-C^{9'}-C^{8a})$ minus 180° − will be used:

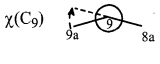


$$\chi(C^9) = [\tau(C^{9a}-C^9-C^{9'}-C^{8a}) \text{ MOD } 360°] - 180° \quad (2)$$

$$\chi(C^{9'}) = [\tau(C^{9a'}-C^9-C^{9'}-C^{8a'}) \text{ MOD } 360°] - 180° \quad (3)$$

In *syn*-pyramidalized double bonds, the pyramidalization angles $\chi(C^9)$ and $\chi(C^{9'})$ have identical signs, whereas in *anti*-pyramidalized double bonds they have opposite signs.

The degree of nonplanarity of the tricyclic moieties may be measured by the dihedral angles A−B and C−D of the least-squares-planes defined by the carbon atoms of the peripheral benzene rings.

### 1.2 Types of Conformations

The classification scheme adopted for the conformational types of bistricyclic enes is given in Table 1. The schematic projections along the $C^9=C^{9'}$ bond should not be confused with Newman projections of the central double bond. The lines represent the peripheral benzene rings of the tricyclic moieties.

Table 1. Conformational types of bistricyclic enes

| | | |
|---|---|---|
| **p** | planar conformation |  |
| $\mathbf{t}_\perp$ | orthogonally twisted conformation |  |
| **t** | twisted conformation |  |
| **a** | *anti*-folded conformation |  |
| **s** | *syn*-folded conformation |  |
| **f** | folded conformation with a planar (or nearly planar) second moiety |  |
| **ta** | twisted/*anti*-folded conformation |  |
| **ts** | twisted/*syn*-folded conformation |  |
| **tf** | twisted/folded conformation |  |
| **at** | *anti*-folded/twisted conformation |  |
| **au** | *anti*-folded conformation with unequal degrees of folding |  |
| **st** | *syn*-folded/twisted conformation |  |
| **su** | *syn*-folded conformations with unequal degrees of folding |  |
| **ft** | folded/twisted conformation |  |
| **pt** | planar central ethylene group with propeller twisted bistricyclic moieties |  |

In the cases where two out-of-plane modes are combined, their order of listing is used to designate the dominant mode. Thus, **ta** is closer to a twisted conformation, while **at** is closer to an *anti*-folded conformation. The symbols **au** and **su** describe unequally folded conformations close to *anti*- and *syn*-folded conformations (**a** and **s**, respectively). In the same spirit, symbols **tau**, **tsu**, **aut**, and **sut** may be defined; however, in this work, the shorter symbols **tf** and **ft** will be preferred for conformations of these types. It should be noted that this classification according to conformation types is empirical and qualitative.

### 1.3 Chirality

The helicity of the central double bond in twisted conformations of **1** introduces an inherently chiral structural element.[86] The chirality sense, or helicity, defined by the sign of the pure ethylenic twist **ω** (vide infra), is indicated by subscripts *P* and *M*, following the Klyne−Prelog convention (Figure 2).[87] This chirality of the central ethylene group vanishes in planar conformations (ω = 0° or 180°) and in orthogonally twisted conformations (ω = ±90°).

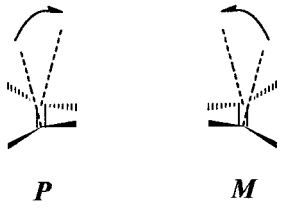


Figure 2. Definition of helicity in twisted central double bonds

In substituted bistricyclic enes, the folding of the tricyclic moiety introduces another, independent element of chirality,[88] reminiscent of a tripodal unit.[86] The assignment of chirality sense (configuration) for a tripodal unit requires two rules: a sequence rule and a conversion rule (or assignment rule), as provided by the Cahn Ingold Prelog (CIP) system.[86,89] In this work, the atom $C^9$ is chosen to define the center of the tripod, and the atoms $C^1$, $C^8$, and $C^{9'}$ define the "ligands" in the given sequence, assuming relative priorities X > C and R > H. This is in agreement with the CIP rules, which allow ranking of the three tree-graph ligands of $C^9$, based on the atoms three and four bonds from the center:[86]

$C^{9a}${C[**X**(C), C(C,H)], C[C(C,*R*), H]} >
$C^{8a}${C[**X**(C), C(C,H)], C[C(C,*H*), H]} >
$C^{9'}${C[**C**(Y,C), C(C,H)], C[C(Y,C), C(C,H)]}

The assignment of chirality sense − *R* or *S* − for substituted, folded tricyclic moieties is illustrated in Figure 3. Note that unsubstituted folded moieties are achiral, but nevertheless may be assigned handedness in a labeled atom sense.

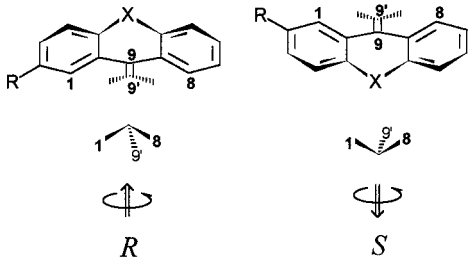


Figure 3. Assignment of chirality sense − *R* or *S* − for substituted, folded tricyclic moieties

### 1.4 Conformations and Point Group Symmetry

Combination of the above classification schemes and descriptors with a symmetry analysis based on the point groups leads to a detailed classification of the conformations, symmetry, and chirality of overcrowded homomerous bistricyclic aromatic enes. The results are summarized in Table 2. A preliminary classification was presented in ref.[7]

In Table 2, the homomerous unsubstituted and disubstituted classes are arranged in columns. Each of the basic conformation − **p**, $\mathbf{t}_\perp$, **t**, **a**, **s**, and **f** − is listed in a separate block. Conformational symbols and the point group symmetry are given, along with the chirality or achirality of the conformation. The *E* and *Z* isomers, the helicity of the central double bond (*P*, *M*), and the chirality of the (substituted) folded moieties (*R*, *S*) are indicated by subscripts. For each of the basic conformations the highest point group is listed first, followed by the subgroups. In cases where the point group symmetry, in addition to the basic conformational mode, allows twisting, *anti*-folding, or *syn*-folding, this is indicated using symbols for mixed conformations − **ta**, **at**, **ts**, **st**, **au**, **su**, and **f**. Note that, from a symmetry point

Table 2. Conformations, symmetry, and chirality of homomerous bistricyclic aromatic enes (**1**, X = Y)

| Unsubstituted[a] R = R' = H | | 2,2'-Disubstituted[a] R = R' | |
|---|---|---|---|
| **p**-$D_{2h}$ | achiral | [*E*: $C_{2h}$ (*x*); *Z*: $C_{2v}$ (*y*)][b] | |
| **p**-$C_{2v}$ (*z*) | achiral | [$C_s$ (*yz*)][b] | |
| **p**-$C_{2h}$ (*x*) | achiral | $\mathbf{p}_E$-$C_{2h}$ (*x*) | achiral |
| **p**-$C_{2v}$ (*y*) | achiral | $\mathbf{p}_Z$-$C_{2v}$ (*y*) | achiral |
| **p**-$C_s$ (*yz*) | achiral | $\mathbf{p}_E$-$C_s$ (*yz*) | achiral |
| | | $\mathbf{p}_Z$-$C_s$ (*yz*) | achiral |
| **pt**-$C_{2h}$ (*z*) | achiral | [*E*: $C_1$; *Z*: $C_s$ (*xy*)][b] | |
| $\mathbf{t}_\perp$-$D_{2d}$ | achiral | [*E*: $C_2$ (*x*); *Z*: $C_2$ (*y*)][b] | |
| $\mathbf{t}_\perp$-$C_{2v}$ (*d*)[c] | achiral | [*E*: $C_2$ (*x*); *Z*: $C_2$ (*y*)][b] | |
| $\mathbf{t}_\perp$-$C_s$ (*d*)[d] | achiral | [$C_1$][b] | |
| $\mathbf{t}_{\perp PM}$-$S_4$ (*z*) | *meso*[e] | [*E*: see $C_2$ (*x*); *Z*: see $C_2$ (*y*)][b] | |
| $\mathbf{t}_P$-$D_2$ | *chiral* | [*E*: $C_2$ (*x*); *Z*: $C_2$ (*y*)][b] | |
| $\mathbf{t}_P$-$C_2$ (*z*) | *chiral* | [$C_1$][b] | |
| $\mathbf{ta}_P$-$C_2$ (*y*) | *chiral* | [$C_1$][b] | |
| | | $\mathbf{ta}_{Z\text{-}RPR}$-$C_2$ (*y*) | *chiral* |
| $\mathbf{ts}_P$-$C_2$ (*x*) | *chiral* | $\mathbf{ts}_{E\text{-}RPR}$-$C_2$ (*x*) | *chiral* |
| | | [$C_1$][b] | |
| **a**-$C_{2h}$ (*y*) | achiral | (*E*: $C_i$; *Z*: $C_2$ (*y*)][b] | |
| **a**-$C_i$ | achiral | $\mathbf{a}_{E\text{-}RS}$-$C_i$ | *meso*[e] |
| | | [*Z*: $C_1$][b] | |
| $\mathbf{at}_P$-$C_2$ (*y*) | *chiral* | [*E*: $C_1$][b] | |
| | | $\mathbf{at}_{Z\text{-}RPR}$-$C_2$ (*y*) | *chiral* |
| **au**-$C_s$ (*xz*) | achiral | [$C_1$][b] | |
| **s**-$C_{2v}$ (*x*) | achiral | [*E*: $C_2$ (*x*); *Z*: $C_s$ (*xy*)][b] | |
| **s**-$C_s$ (*xy*) | achiral | [*E*: $C_1$][b] | |
| | | $\mathbf{s}_{Z\text{-}RS}$-$C_s$ (*xy*) | *meso*[e] |
| $\mathbf{st}_P$-$C_2$ (*x*) | *chiral* | $\mathbf{st}_{E\text{-}RPR}$-$C_2$ (*x*) | *chiral* |
| | | [*Z*: $C_1$][b] | |
| **su**-$C_s$ (*xz*) | achiral | [$C_1$][b] | |
| **f**-$C_s$ (*xz*) | achiral | [$C_1$][b] | |
| $\mathbf{ft}_P$-$C_1$ | *chiral* | $\mathbf{ft}_{E\text{-}RPR}$-$C_1$ [f] | *chiral* |
| | | $\mathbf{ft}_{E\text{-}RPS}$-$C_1$ [g] | *chiral* |
| | | $\mathbf{ft}_{Z\text{-}RPR}$-$C_1$ [g] | *chiral* |
| | | $\mathbf{ft}_{Z\text{-}RPS}$-$C_1$ [f] | *chiral* |

[a] For chiral conformations, only one enantiomer (*P*) is given. Conformations with $C_1$ symmetry are represented by **ft**, listed at the bottom of the table. − [b] See this point group further down in this column. − [c] In this orientation of the point group $C_{2v}$, the reflection planes are the diagonal planes $y = x$ and $y = -x$, respectively. − [d] The reflection plane is the plane $y = x$. − [e] The two moieties have opposite chirality sense. − [f] The relative direction of folding of the two moieties is *syn*. − [g]The relative direction of folding of the two moieties is *anti*.

of view, the magnitude of the contributions of two modes in a mixed conformation is irrelevant. The point group and symmetry properties are identical. However, the conformations may look significantly different (vide infra). Any conformation combining three modes (**t**, **a**, and **s**) of out-of-plane deformation has point group $C_1$.

### 1.5 Dynamic Stereochemistry

In bistricyclic enes, three fundamental dynamic processes have been observed:

(a) *E,Z* isomerization as illustrated in Figure 4

(b) enantiomerization or conformational inversion: inversion of the helicity in twisted **1** (Figure 5), or inversions of the boat conformations in the central rings of *anti*-folded **1** (Figure 6);

(c) *syn*, *anti* isomerization (**s** → **a**) as illustrated in Figure 7.

It should be noted that enantiomerization and conformational inversion may also be considered in processes (a) and (c).

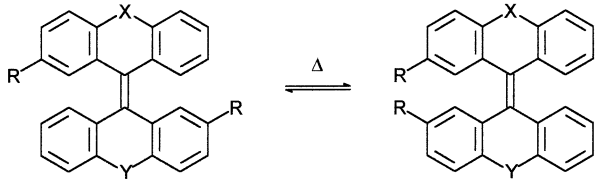


Figure 4. Thermal *E,Z* isomerization of 2,2′-disubstituted bistricyclic enes

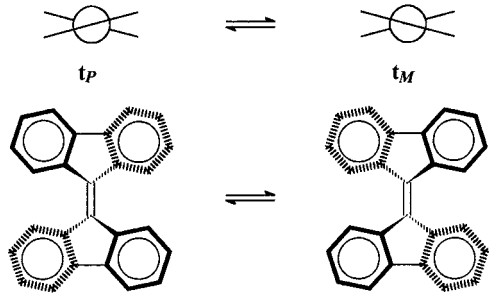


Figure 5. Enantiomerization of twisted bistricyclic enes

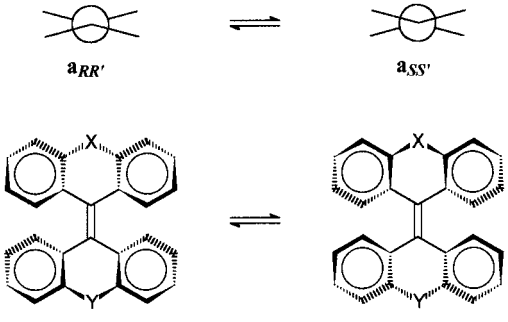


Figure 6. Conformational inversion of *anti*-folded bistricyclic enes

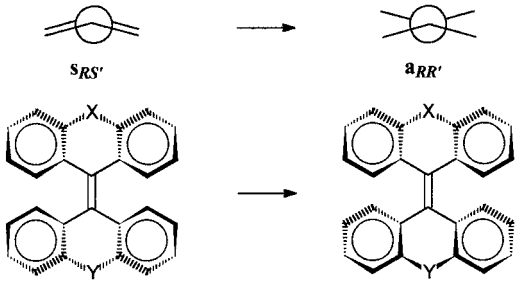


Figure 7. The *syn,anti* isomerization of bistricyclic enes

The dynamic stereochemistry of bistricyclic aromatic enes has been reviewed recently.[11] The dynamic processes of bifluorenylidenes and of the homomerous bistricyclic enes with central six-membered rings have been extensively studied.[68,71,77,90–105] The experimental Gibbs energies of activation for thermal *E,Z* isomerization [$\Delta G_c^{\ddagger}(E,Z)$] of disubstituted bistricyclic enes are reviewed in Table 3. Table 4 summarizes the Gibbs energies of activation for thermal en-

Table 3. Experimental Gibbs energies of activation for thermal *E,Z* isomerizations [$\Delta G_c^{\ddagger}(E,Z)$] of disubstituted bistricyclic enes

| Parent system | Bridges X, Y | Substituents | $\Delta G_c^{\ddagger}(E,Z)$ [kcal/mol] | Method |
|---|---|---|---|---|
| **2** | – | 2,2′-di-Me | 25.0 | DNMR [67] |
| **3** | O | 2,2′-di-Me | 17.1 | DNMR [68] |
| **4** | CO | 2,2′-di-Me | 20.0 | DNMR [96,98] |
| **8** | $NCH_3$ | 2,2′-di-Me | 20.8 | DNMR [71] |
| **10** | $CH_2$ | 2,2′-di-Me | 23.8 | DNMR [77] |
| **9** | S | 2,2′-di-Me | 27.4 | kinetic[a] [103] |
| **2** | – | 2,2′-di-F | >25 | DNMR [93] |
| **2** | – | 2,2′-di-$NH_2$ | 25 | kinetic[b] [90] |
| **3** | O | 2,2′-di-*i*Pr | 17.5 | DNMR [68] |
| **3** | O | 2,2′-di-*t*Bu | 18.0 | DNMR [68] |
| **3** | O | 2,2′-di-*O*Me | 18.4 | DNMR [92] |
| **4** | CO | 2,2′,3,3′-tetra-Me-6,6′-Br | 20.3 | DNMR [98] |
| **4** | CO | 2,2′-di-*O*-*i*Pr | 21.0 | DNMR [92] |
| **4** | CO | 2,2′-di-$CF_3$ | 21.5 | DNMR [96,98] |
| **8** | $NCH_3$ | 2,2′-di-Et | 21.4 | DNMR [71] |
| **8** | $NCH_3$ | 2,2′-di-*t*Bu | 21.8 | DNMR [71] |
| **8** | $NCH_3$ | 2,2-di-$OCH_3$–6,6′-Cl | 20.3 | DNMR [71,96] |
| **12** | – | 2,3:2′,3′-dibenzo | 23.5 | DNMR [94] |
| **13** | CO | 2,2′-di-Me, 6,7:6′,7′-dibenzo | 21.6 | DNMR [98] |
| **14** | CO | 2,2′-di Me, 5,6:5′,6′-dibenzo | 22.7 | DNMR [98] |
| **15** | CO | 2-Me | 14.6 | DNMR [99] |
| **16** | $CH_2$ | 2,2′-di-Me, 6,7:6′,7′-dibenzo | 24.0 | DNMR [77] |
| **2** | – | 1,1′-di-F | >22.4 | DNMR [93,94] |
| **2** | – | 1,1′-di-Cl | [c] | DNMR [93] |
| **2** | – | 1,1′-di-Me | 19.0 | DNMR [93] |
| **2** | – | 1,1′-di-$CO_2$Me | 20.1 | DNMR [91,92] |
| **2** | – | 1-$CO_2$Me, 1′-$CO_2$-*I*Pr | 20.9 | DNMR [91,92] |

[a] Isomerization kinetics followed by HPLC. – [b] Activation energy $E_A$ from *E,Z* isomerization kinetics, followed by column chromatography and photometry. – [c] A coalescence point $T_c \approx 140$ °C was reported, see ref.[93]

Table 4. Experimental Gibbs energies of activation for thermal enantiomerizations and conformational inversions [$\Delta G_c^{\ddagger}$(inv)] of bistricyclic enes

| Parent system | Bridges X, Y | Substituents | $\Delta G_c^{\ddagger}$(inv) [kcal/mol] | Method |
|---|---|---|---|---|
| **2** | – | 2-$CH(CH_3)_2$ | 10.5 | DNMR [67] |
| **3** | O | 2,2′-di-$CH(CH_3)_2$ | 17.7 | DNMR [68] |
| **10** | $CH_2$ | 2,2′-di-$CH_3$ | 23.4 | DNMR [77] |
| | $C(CH_3)_2$ | | >25.8 | DNMR [77] |
| **9** | S | 2,2′-di-$CH_3$ | 27.4 | kinetic[a] [103] |
| **9** | S | 2-$CH_3$ | 27.3, 27.4 | kinetic[b] [16,103] |
| **9** | S | 2,2′-di-$CH_2$OH, 7,7′-di-$OCH_3$ | 26.7 | kinetic[b] [105] |
| | S, O | 2-$CH_3$ | <20 | kinetic[b] [103] |
| | S, $C(CH_3)_2$ | 2-$CH_3$ | 25.1 | kinetic[b] [103] |
| | S, $NCH_3$ | 2-$CH_3$ | 21.3 | kinetic[b] [16,103] |
| | $CH_2$ | 2,2′-di-Me, 6,7:6′,7′-dibenzo | 23.1 | DNMR [77] |
| | S | 1,2-benzo | 28.6 | kinetic[b] [104] |
| | S | 1,2-benzo | 28.4 | kinetic[b] [16] |
| | O, S | 1,2-benzo | 26.7 | kinetic[b] [16] |
| | S, O | 1,2-benzo | 25.9 | kinetic[b] [16] |
| **17** | – | 2,2′-di-CONH-CHMePh | 11.5 | DNMR [101] |
| **18** | – | 2,2′-tethered | 12.0 | DNMR [100,101] |
| **19** | – | 2,2′,7,7′-tetra-*t*Bu | 15.0 | DNMR [102] |
| **2** | – | 1,1′-di-$CO_2$-*i*Pr | 21.0 | DNMR [91,92] |
| **2** | – | 1-$CO_2$Me, 1′-$CO_2$*i*Pr | 20.8 | DNMR [91,92] |
| **3** | O | 1,1′,3,3′-tetra-$OCH(CH_3)_2$ | 24.1 | DNMR [92] |
| **4** | CO | 1,1′-di-$OCH(CH_3)_2$ | 25.8 | DNMR [92] |

[a] Isomerization kinetics followed by HPLC. – [b] Racemization kinetics followed by polarimetry.

antiomerizations and conformational inversions [$\Delta G_c^{\ddagger}$(inv)] of representative homomerous and heteromerous bistricyclic enes.

The dynamic stereochemistry of bifluorenylidenes has been a controversial issue[11,91−93,102,106,107] since the seminal communication in 1970 on the conformational behavior of 1,1′-bis(alkoxycarbonyl)bifluorenylidenes.[91] These overcrowded diesters showed low barriers ($\Delta G_c^{\ddagger}$ = 20−21 kcal/mol) both for *E,Z* isomerizations and for conformational inversions.[91] The conformational behavior of 1,1′-disubstituted bifluorenylidenes was found to be strongly substituent-dependent.[91,93] In 1,1′-difluoro- and 2,2′-difluoro-9*H*-bifluoren-9-ylidene, $\Delta G_c^{\ddagger}(E,Z)$ is > 25 kcal/mol.[91,93] In 2,2′-dimethyl-9*H*-bifluoren-9-ylidene, which closely resembles the parent system **2**, $\Delta G_c^{\ddagger}(E,Z)$ is 25.2 kcal/mol.[67] (*E*)- and (*Z*)-2,2′-diamino-9*H*-bifluoren-9-ylidene have been separated by column chromatography, and the Arrhenius activation energy of their interconversion determined to be 25 kcal/mol.[90] In (*E,Z*)-11,11′-bis(11*H*-benzo[*b*]fluoren-11-ylidene) (**12**), the lower barrier of $\Delta G_c^{\ddagger}(E,Z)$ = 23.5 kcal/mol, has been attributed to an enhanced stabilization of an orthogonal diradical transition state.[95]

The free energies of activation for thermal enantiomerization of bifluorenylidenes are remarkably low, and an attempt to resolve them has failed.[108] The enantiomerization barrier of 2-isopropyl-9*H*-bifluoren-9-ylidene is 10.5 kcal/mol.[67] Barriers of 11.5 kcal/mol for rapid equilibration between two diastereomers of *N,N′*-bis[(*R*)-1-phenylethyl]-(*Z*)-9*H*-bifluoren-9-ylidene-2,2′-dicarboxamide (**17**) and 12.0 kcal/mol for "racemization" of a chiral (*Z*)-2,2′-tethered bifluorenylidene **18** have been reported.[100,101] A "racemization" barrier of $\Delta G_c^{\ddagger}$(inv) = 15.0 kcal/mol was reported for a 4,4′-bis(cyclohepta[*def*]fluorenylidene).[102] The higher barriers for "racemization" of bifluorenylidenes with additional steric constraints[100−102] do not reflect the intrinsic enantiomerization barrier of the parent hydrocarbon **2**.

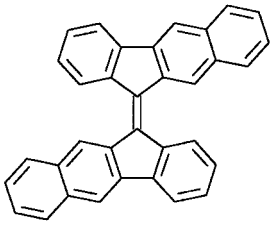

(*E*)-**12**

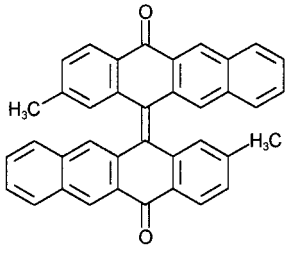

(*E*)-**13**

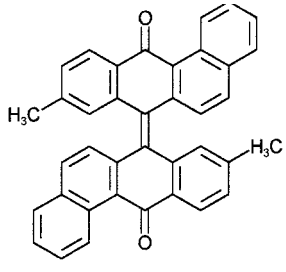

(*E*)-**14**

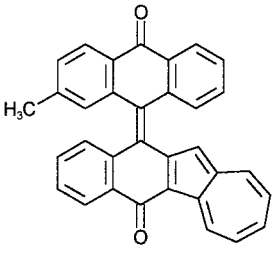

(*E*)-**15**

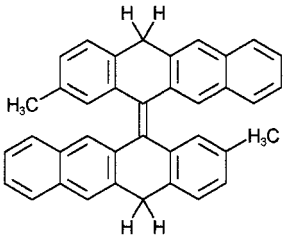

(*E*)-**16**

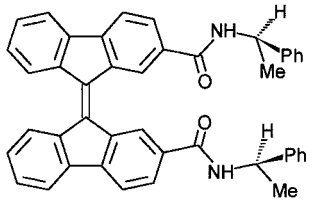

**17**

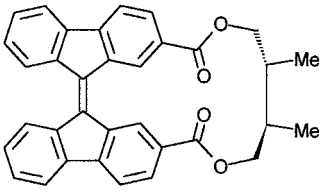

**18**

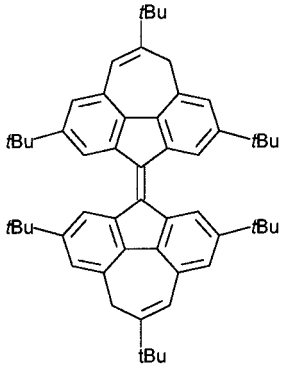

**19**

The low barriers associated with the *E,Z* isomerization of the bistricyclic enes with central six-membered rings [$\Delta G_c^{\ddagger}(E,Z)$ = 14.6−27.4 kcal/mol] were interpreted predominantly in terms of ground-state destabilization due to steric strain and overcrowding, rather than in terms of stabilization of the biradical transition state.[96,97] These barriers are considerably lower than the *E,Z* isomerization barriers for substituted tetraarylethylenes.[109] For example, the Arrhenius activation energy for thermal *E,Z* isomerization of 1,2-diphenyl-1,2-bis(4-methylphenyl)ethylene is 35.3 kcal/mol.[109]

The increase in $\Delta G_c^{\ddagger}(E,Z)$ with the bulkiness of the 2,2′-substitutents (Me < Et < *i*Pr < *t*Bu) in the *N,N′*-dimethylbiacridane (**8**) (**1**, X,Y: NMe)[71] and dixanthylene (**3**) (**1**, X,Y: O)[68] series was interpreted in terms of R(2)···H(2′)-type secondary steric interactions in the folded/twisted transition state.[68,71] This indicated that the orthogonally twisted biradical transition state is not the highest transition state in an *E,Z* isomerization.[68,71]

In the bianthrone (**4**) and the methylene-bridged bistricyclic ene (**10**) series, $\Delta G_c^{\ddagger}(E,Z)$ values are not lowered by benzannulation of the parent systems (Table 3). In the dibenzobianthrone analogs **13** and **14**, $\Delta G_c^{\ddagger}(E,Z)$ values were even somewhat higher than that of 2,2′-dimethyl-**4** [21.5 kcal/mol (**13**) and 22.7 kcal/mol (**14**) versus 20.2 kcal/mol].[98] This benzoannulation effect ruled out the orthogonally twisted biradical conformations as the highest transition states for the *E,Z* isomerizations in **1** with central six-membered rings (in contrast to the situation in bifluorenylidenes).[98] It is interesting to note the significantly lower $\Delta G_c^{\ddagger}(E,Z)$ value of 14.6 kcal/mol for the bianthrone analog **15**, bearing a sterically less demanding azulene moiety.[99]

The barriers for conformational inversion and for *E,Z* isomerization of 2,2′-disubstituted dixanthylenes, dithioxanthylenes, and methylene-bridged **10** are identical, within experimental error.[68,77,103] This argues in favor of a common highest transition state for both dynamic processes.[68,77]

Feringa et al. have shown that, for a series of substituted bistricyclic enes **1**: X = S, Y = S, $C(CH_3)_2$, $NCH_3$, and O, the racemization barriers (27.4, 25.1, 21,3, and < 20.0 kcal/mol, respectively) depend upon the aryl−Y bond lengths.[103] It should be noted that, in these 2-methyl-substituted bistricyclic enes, a racemization may be due to a conformational inversion or to an *E,Z* isomerization.[103] The high barrier for the dithioxanthylene (**9**) derivatives − 27.4 kcal/mol − permitted a separation of the three stereoisomers (the achiral $\mathbf{a}_{E\text{-}RS'}$, and the enantiomers $\mathbf{a}_{Z\text{-}RR'}$ and $\mathbf{a}_{Z\text{-}SS'}$).[103] The *syn* ⇄ *anti* isomerization barrier of bi-5*H*-dibenzo[*a*,*d*]cyclohepten-5-ylidene (**11**) was found to be even higher − $\Delta G^{\ddagger}_{347}$ = 36.4 kcal/mol − in a bistricyclic ene with central seven-membered rings.[73]

A PM3 study of the **a** ⇄ **t** conformational isomerization of bianthrone (**4**) has previously been reported.[110,111] PM3 results on bifluorenylidene (**2**), dixanthylene (**3**), diselenoxanthylene (**1**, X,Y: Se), ditelluroxanthylene (**1**, X,Y: Te), the methylene-bridged ene **10**, and the isopropylidene-bridged **1** (**1**, X,Y: $C(CH_3)_2$) have been reported.[7,77,112] Two earlier MINDO/3 studies of the **a** ⇄ **t** isomerization of bifluorenylidene and bianthrone, using partially optimized structures with fixed bond lengths and angles and planar benzene rings, have been reported.[113,114] Recently, ab initio DFT calculations on twisted bifluorenylidene (**2**) and *anti*-folded bianthrone (**4**) (B3LYP/6−31G*), and of *anti*- and *syn*-folded vinylidene-bridged **1** (**1**, X,Y: C=$CH_2$) (B3LYP/6−31G*//HF/6−31G*) have been reported.[21,115] A PM3 study of the conformational space of the heteromerous fluorenylidene-xanthene (**1**, X: O, Y: −) has been reported very recently.[116]

### 1.6 Methods

The geometries of all conformations were fully optimized using the semiempirical method PM3[60] as implemented in the program MOPAC6.[117,118] Optimization criteria were increased and a gradient norm below 0.1 enforced in order to secure reproducible results.[119] Vibrational frequencies were calculated for all conformations.[120] The conformational space was searched comprehensively for conformations of lower symmetry, in particular for transition states of dynamic processes. Internal coordinates pertaining to twisting, folding, bending, and the passage of the two hydrogen atoms in a fjord region were incrementally raised or decreased in 2° steps. The other geometrical parameters were optimized at each point. All minima and maxima found in these searches were used as starting points for optimizations.[121] Intrinsic reaction coordinates (IRC)[122] were calculated to identify unambiguously the reactant and product of each transition state, verifying that no intermediates were missing among the various potential conformations and in order to elucidate the mechanisms of the dynamic stereochemistry in detail. For the orthogonally twisted biradicals, no IRC calculations were carried out, because these calculations would have been excessively demanding.

## 2. Bifluorenylidene

Bifluorenylidene (**2**) (**1**, X,Y: −), the smallest overcrowded bistricyclic aromatic ene, is a unique case among the homomerous bistricyclic enes, because of its central 5-membered rings. This topology introduces a bias towards planarity of the tricyclic moieties, while at the same time rendering these tricyclic moieties sterically less demanding, especially in twisted conformations.[2] Bifluorenylidenes are the only known homomerous bistricyclic aromatic enes with a twisted global minimum conformation.[35,64−67] The 2D structure and atom labeling is shown in Figure 8.

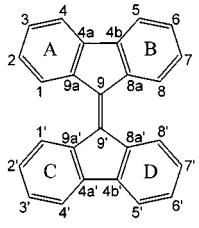


Figure 8. Structure and atom labeling of bifluorenylidene (**2**)

### 2.1 Conformers and Transition States

For bifluorenylidene (**2**), 4 minimum energy conformations, 5 transition states, and 2 higher order saddle points were computed. The results of the PM3 calculations are summarized in Table 5. The conformations are listed in order of increasing energy. The shorthand symbols for the various conformations are derived from the conformational type (see Table 1). Transition states and higher order saddle points are indicated by square brackets ([ ]) and double square brackets ([[ ]]), respectively. Some 3D projections of minima and transition states are shown in Figure 9 and Figure 10, respectively.

The global minimum twisted/*anti*-folded conformation **ta** has a pure ethylenic twist of ω = 31.5° and is slightly folded, with A−B = 3.8°. The nonbonding distance $H^8\cdots H^{8'}$ (1.78 Å) is highly overcrowded (22% overlap of the van der Waals radii).[123]

The *anti*-folded/twisted conformation **at** is a local minimum with a relative energy of 4.3 kcal/mol and characterized by a high degree of folding (A−B = 20.9°), and considerably less twisting (ω = 11.4°). This structure has the shortest double bond of all bifluorenylidene conformations (1.353 Å). The nonbonding distance $H^8\cdots H^{8'}$ (1.71 Å) is highly overcrowded (26% overlap).

The $C_{2h}$-symmetric, *anti*-folded conformation **a** is a local minimum with a relative energy of 4.8 kcal/mol, 0.5 kcal/mol higher than that for the **at** conformation. The fluorenylidene moieties are folded by A−B = 20.8°. There is no pure ethylenic twist ω. The atoms of the central double bond are *anti*-pyramidalized, with χ = ∓7.9°. The fjord

Table 5. Conformations of bifluorenylidene (**2**) calculated by PM3

| Conformation | | | [a] | PM3 $\Delta H_f°$ [kcal/mol] | $\Delta\Delta H_f°$ [kcal/mol] | ω[b] [°] | Folding A−B [°] | Bond $C^9=C^{9'}$ | χ($C^9$) | $C^1\cdots C^{1'}$ $C^8\cdots C^{8'}$ | $C^1\cdots H^{1'}$ $C^8\cdots H^{8'}$ | $H^1\cdots H^{1'}$ $H^8\cdots H^{8'}$ |
|---|---|---|---|---|---|---|---|---|---|---|---|---|
| **ta** | twisted/ *anti*-folded | **ta**-$C_2$ (y) | Min | 140.7 | 0.0 | 31.5 | 3.8 | 1.357 | −2.4 | 3.06<br>3.16 | 2.50<br>2.39 | 2.29<br>1.78 |
| **t** | twisted | **t**-$D_2$ | Min | 140.9 | 0.2 | 30.2 | 2.5 | 1.358 | 0.0 | 3.08 | 2.36 | 1.88 |
| [**ta-t**] | | **ta**-$C_2$ (y) | TS | 140.9 | 0.2 | 30.3 | 2.5 | 1.358 | −0.4 | 3.07<br>3.09 | 2.37<br>2.36 | 1.94<br>1.86 |
| **at** | *anti*-folded/ twisted | **ta**-$C_2$ (y) | Min | 145.0 | 4.3 | 11.4 | 20.9 | 1.353 | −9.2 | 2.92<br>3.14 | 2.45<br>2.37 | 2.37<br>1.71 |
| **a** | *anti*-folded | **a**-$C_{2h}$ (y) | Min | 145.5 | 4.8 | 0.0 | 20.8 | 1.354 | −7.9 | 2.99 | 2.29 | 1.86 |
| [**at-a**] | | **ta**-$C_2$ (y) | TS | 145.5 | 4.8 | 0.8 | 20.8 | 1.354 | −7.9 | 2.98<br>2.99 | 2.29<br>2.29 | 1.88<br>1.84 |
| [**ta-at**] | | **ta**-$C_2$ (y) | TS | 145.6 | 4.9 | 23.3 | 16.6 | 1.357 | −8.9 | 2.90<br>3.36 | 2.51<br>2.52 | 2.55<br>1.58 |
| [**s**] | *syn*-folded | **s**-$C_{2v}$ (x) | TS | 149.0 | 8.4 | 0.0 | 22.5 | 1.355 | 22.2 | 3.11 | 2.51 | 1.64 |
| ‖[**a-s**]‖ | | **su**-$C_s$ (xz) | 2 | 149.3 | 8.6 | 0.0 | 11.0<br>30.3[c] | 1.356 | 15.3<br>22.8[c] | 3.10 | 2.66<br>2.25[c] | 1.66 |
| [$\mathbf{t}_\perp$] | 90°-twisted | $\mathbf{t}_\perp$-$D_{2d}$ | TS | 165.9 | 25.2 | 90.0 | 0.0 | 1.437 | 0.0 | 4.37 | 4.09 | 4.07 |
| ‖[**p**]‖ | planar | **p**-$D_{2h}$ | 3 | 170.2 | 29.6 | 0.0 | 0.0 | 1.375 | 0.0 | 3.07 | 2.18 | 1.16 |

[a] Minimum (Min), transition state (TS), or number of imaginary frequencies of a higher order saddle point. − [b] Pure twist of central ethylene group. − [c] Refers to second moiety.

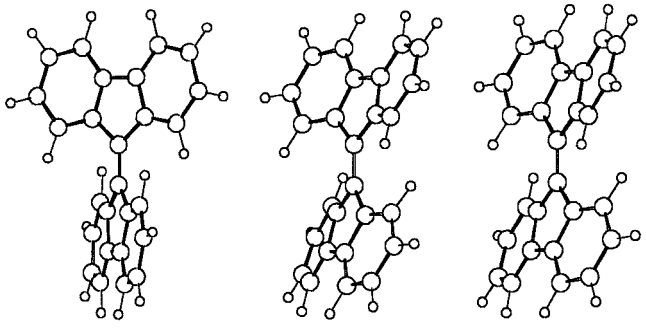

Figure 9. 3D projections of the twisted/*anti*-folded global minimum conformation **ta** (left), the *anti*-folded/twisted local minimum conformation **at** (center), and the *anti*-folded local minimum conformation **a** (right) of bifluorenylidene (**2**)

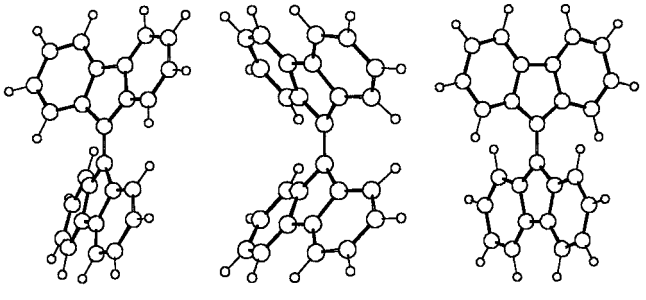

Figure 10. 3D projections of the transition states [**ta-at**] (left), [**s**] (center), and [$\mathbf{t}_\perp$] (right) of bifluorenylidene (**2**)

regions are highly overcrowded: C···C = 2.99 Å, C···H = 2.29 Å, and H···H = 1.86 Å (13%, 20%, and 19% overlap).

The transition state [**ta-at**] has a relative energy of 4.9 kcal/mol, and is highly twisted (ω = 23.3°) and folded (A−B 16.6°). The ethylene group bond angles $C^{9a}-C^9-C^{9'}$ (123.2°) and $C^{8a}-C^9-C^{9'}$ (132.6°) differ by 9.4°, indicating a high degree of in-plane bending. In this structure, the differences between corresponding geometrical parameters on the left- and right-hand side of the molecule are the largest observed in all the conformations of bifluorenylidene. The nonbonding distances are $C^1\cdots C^{1'}$ = 2.90 Å versus $C^8\cdots C^{8'}$ = 3.36 Å, and $H^1\cdots H^{1'}$ = 2.55 Å versus $H^8\cdots H^{8'}$ = 1.58 Å. The hydrogen atoms $H^8$ and $H^{8'}$ are in the process of passing one another at a distance reflecting 31% overlap. This is the "edge passage"[50,104] where the two bucking hydrogen atoms of one fjord region pass one another.

The twisted conformations **ta** and **t**, the *anti*-folded/twisted conformation **at**, and the *anti*-folded conformation **a** are part of an isomerization cycle, which also involves the corresponding enantiomeric conformations and is the basis of the low energy thermal enantiomerization mechanism of bifluorenylidene illustrated in Figure 11. The connectivity of the various transition states and minima was verified by IRC calculations.

The *syn*-folded conformation [**s**] with $C_{2v}$ symmetry is a transition state for an alternative enantiomerization of the twisted conformation **t**, with a barrier of 8.4 kcal/mol, shown in Figure 12. The folding dihedral A−B is 22.5° and *syn*-pyramidalization χ = 22.2°. In this transition state, both pairs of bucking hydrogen atoms pass one another simultaneously at a distance of 1.64 Å, (29% overlap).[123]

The conformation ‖[**a-s**]‖ is the highest point on the $C_s$-symmetric minimum energy pathway from **a** to [**s**]. However, this stationary point is a second order saddle point with two imaginary frequencies, and therefore does not qualify as transition state.[124]

The orthogonally twisted $D_{2d}$ conformation [$\mathbf{t}_\perp$] is a biradical and the transition state for rotation of **t** about the central double bond. The orthogonal biradical has a relative energy of 25.2 kcal/mol. Both fluorenylidene moieties are planar, and there is no overcrowding in this structure. The transition state [$\mathbf{t}_\perp$] serves as a model for the *E,Z* isomerization in disubstituted bifluorenylidenes (Figure 13). It should be noted that, in disubstituted bifluorenylidenes,

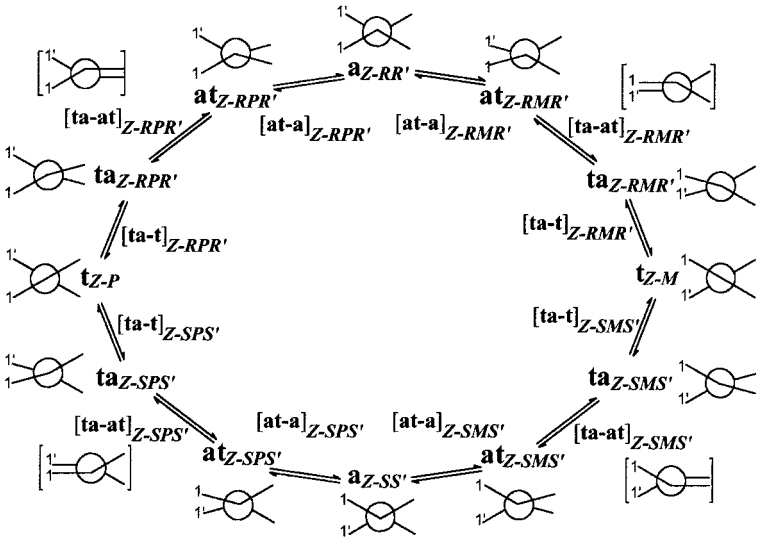


Figure 11. Scheme of the dynamic mechanism for the interconversion of the twisted and *anti*-folded conformations of bifluorenylidene (**2**). Symbolic projections along the $C^9{=}C^{9'}$ bond are given for the minima and the highest transition state [**ta-at**]

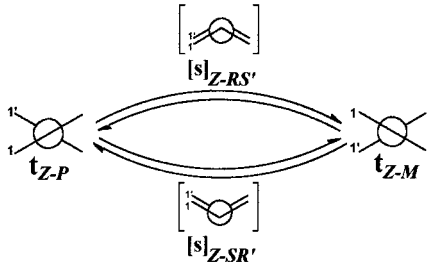


Figure 12. Scheme of an alternative dynamic mechanism for enantiomerization of twisted bifluorenylidene **t** via the *syn*-folded transition state [**s**]

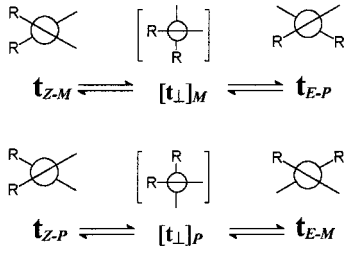


Figure 13. Scheme of the thermal *E,Z* isomerization mechanism in disubstituted bifluorenylidenes

there are two enantiomeric transition states $[t_\perp]_P$ and $[t_\perp]_M$.

The planar $D_{2h}$ conformation ‖[**p**]‖ has a relative energy of 29.6 kcal/mol and can thus be excluded as a transition state for the dynamic stereochemistry of bifluorenylidene. Indeed, this stationary point is not a proper transition state: it has 3 imaginary vibrational frequencies.

### 2.2 Dynamic Stereochemistry of Bifluorenylidene

Figure 14 summarizes the dynamic stereochemistry of bifluorenylidene (**2**), as derived from the PM3 calculations. For simplicity, the conformations **ta** and **t** are represented by **t**. Only the highest transition states and most important intermediates are shown. The most rapid process in the dynamic stereochemistry of bifluorenylidene (**2**) is the enantio-

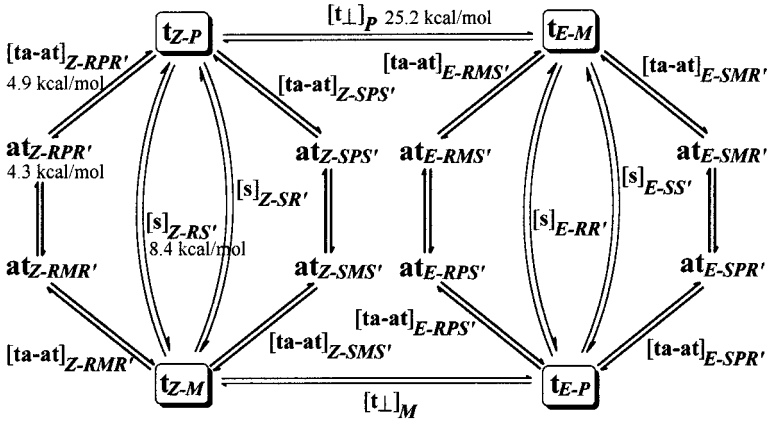


Figure 14. Scenario of the dynamic processes in bifluorenylidene (**2**)

merization of the twisted conformations **t** via the *anti*-folded/twisted intermediates **at** and the highest transition states [**ta-at**] (bold arrows in Figure 14). The barrier of 4.9 kcal/mol is due to the steric requirements of an edge passage. The alternative single-step enantiomerization via [**s**] has a higher barrier (8.4 kcal/mol), due to the simultaneous double edge passage. However, the PM3-calculated barriers for both mechanisms are below the experimental barrier for enantiomerization of 2-isopropyl-9*H*-bifluoren-9-ylidene [$\Delta G^{\ddagger}_{c}$(inv) = 10.5 kcal/mol].[67] The *E,Z* isomerization may proceed in a single step via the orthogonal biradical transition state [$\mathbf{t}_{\perp}$] (25.2 kcal/mol). This is in excellent agreement with the experimentally determined *E,Z* isomerization barrier in 2,2′-dimethyl-9*H*-bifluoren-9-ylidene [$\Delta G^{\ddagger}_{c}(E,Z)$ = 25.0 kcal/mol].[67] In bifluorenylidene, the transition state for *E,Z* isomerization, [$\mathbf{t}_{\perp}$] is much higher and is clearly distinct from the highest transition state for enantiomerization [**ta-at**].

## 3. Dixanthylene

Dixanthylene (**3**) is a representative homomerous bistricyclic aromatic ene with central 6-membered rings and an *anti*-folded global minimum conformation. It is thermochromic and photochromic and has been extensively studied.[45−48,68] The 2D structure and atom labeling is shown in Figure 15.

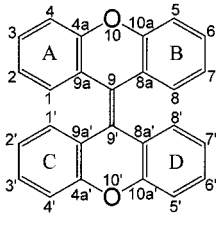


Figure 15. Chemical structure and atom labeling in dixanthylene (**3**)

### 3.1 Conformers and Transition States

For dixanthylene, 3 minima, 3 transition states, and 3 higher order saddle points were identified. The results are summarized in Table 6. 3D projections of the minima and transition states are shown in Figure 16 and Figure 17, respectively.

The global minimum conformation of dixanthylene is the *anti*-folded conformation **a**, with $C_{2h}$ symmetry, a folding dihedral A−B of 40.4° and zero ethylenic twist. In the fjord regions, the nonbonding C···C distance of 2.95 Å indicates

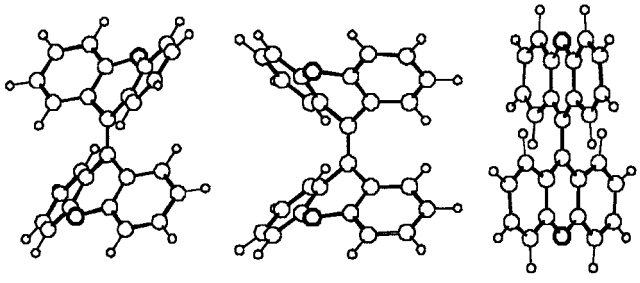

Figure 16. 3D projections of the *anti*-folded global minimum conformation **a** (left), the *syn*-folded local minimum conformation **s** (center), and the twisted local minimum conformation **t** (right) of dixanthylene (**3**)

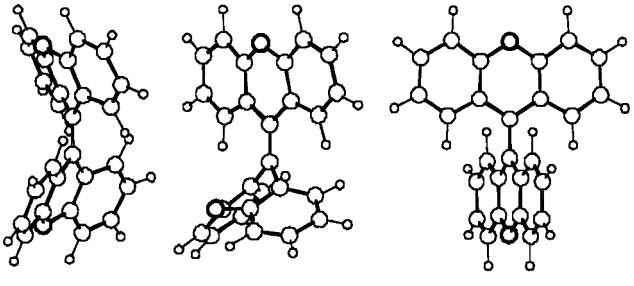

Figure 17. 3D projections of the [**s-t**] (left), [**a-s**] (center) and [$\mathbf{t}_{\perp}$] (right) transition states of dixanthylene (**3**)

Table 6. Conformations of dixanthylene (**3**) calculated by PM3

| Conformation | | | [a] | PM3 $\Delta H_f^{\circ}$ [kcal/mol] | $\Delta\Delta H_f^{\circ}$ [kcal/mol] | ω [b] [°] | Folding A−B [°] | Bond $C^9{=}C^{9'}$ | $\chi(C^9)$ $\chi(C^{9'})$ | $C^1\cdots C^{1'}$ $C^8\cdots C^{8'}$ | $C^1\cdots H^{1'}$ $C^8\cdots H^{8'}$ | $H^1\cdots H^{1'}$ $H^8\cdots H^{8'}$ |
|---|---|---|---|---|---|---|---|---|---|---|---|---|
| **a** | *anti*-folded | **a**-$C_{2h}$ (y) | Min | 65.7 | 0.0 | 0.0 | 40.4 | 1.354 | −4.8 | 2.95 | 2.72 | 2.91 |
| **s** | *syn*-folded | **s**-$C_{2v}$ (x) | Min | 69.8 | 4.0 | 0.0 | 44.0 | 1.353 | 15.6 | 3.03 | 2.53 | 1.72 |
| **t** | twisted | **t**-$D_2$ | Min | 74.4 | 8.7 | 49.2 | 2.3 | 1.386 | 0.0 | 2.98 | 2.58 | 2.61 |
| [**s-t**] | | **ts**-$C_2$ (x) | TS | 75.2 | 9.5 | 44.6 | 26.6 | 1.375 | −4.4 | 3.09 | 2.28<br>2.97 | 2.47 |
| [**a-s**] | | **ft**-$C_1$ | TS | 81.6 | 15.9 | 13.1 | 7.6<br>59.9[c] | 1.365 | 4.9<br>15.9 | 3.06<br>2.92 | 3.17<br>2.18<br>2.75[c]<br>1.90[c] | 2.58<br>1.71 |
| [$\mathbf{t}_{\perp}$] | | $\mathbf{t}_{\perp}$-$D_{2d}$ | TS | 82.0 | 16.3 | 90.0 | 0.0 | 1.460 | 0.0 | 3.91 | 3.61 | 3.62 |
| ‖[**a-s**]‖$_{Cs}$ | | **f**-$C_s$ (xz) | 2 | 82.6 | 16.9 | 0.0 | 0.5<br>59.1[c] | 1.365 | 3.8<br>13.4 | 2.89 | 2.84<br>1.89[c] | 2.06 |
| ‖[**a-t**]‖ | | **ta**-$C_{2h}$ (y) | 2 | 83.5 | 17.8 | 49.3 | 24.9 | 1.385 | −8.4 | 3.35<br>3.39 | 3.50<br>2.50 | 3.91<br>1.50 |
| ‖[**p**]‖ | planar | **p**-$D_{2h}$ | 9 | 206.0 | 140.3 | 0.0 | 0.0 | 1.437 | 0.0 | 2.87 | 1.96 | 0.94 |

[a] Minimum (Min), transition state (TS), or number of imaginary frequencies of a higher order saddle point. − [b] Pure twist of central ethylene group. − [c] Refers to the second moiety.

a high degree of intramolecular overcrowding (14% overlap).[123]

The second minimum is the *syn*-folded $C_{2v}$ conformation **s**, with a relative energy of 4.0 kcal/mol and a folding dihedral A−B of 44.0°. The very short fjord region H···H distance of 1.72 Å indicates a high degree of overcrowding (27% overlap).

The $D_2$-symmetric, twisted conformation **t** is a third minimum, with a relative energy of 8.7 kcal/mol. The central double bond is twisted by ω = 49.2° and is 0.03 Å longer than in the *anti*-folded and *syn*-folded conformations. There is no pyramidalization and no folding; the dihedral A−B of 2.3° is due to a propeller twist. The fjord regions are less overcrowded.

The conformations **s** and **t** interconvert via the transition state [**s-t**], with a relative energy of 9.5 kcal/mol (Figure 18). The central double bond is twisted by ω = 44.6° and the folding dihedral is A−B = 26.6°. In the fjord region, the $C^1\cdots H^{1'}$ distance of 2.28 Å (20% overlap) is much shorter than in **a** and **t**.

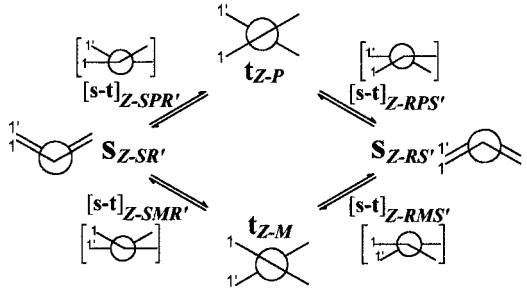


Figure 18. Scheme of the dynamic mechanism of the *syn*-folded to twisted conformational isomerization **s** ⇄ **t** of dixanthylene (**3**)

The conformations **a** and **s** interconvert via the folded/twisted $C_1$-symmetric (type **ft**-$C_1$) transition state [**a-s**], with a relative energy of 15.9 kcal/mol, ethylenic twist ω of 13.1° and folding dihedrals A−B of 7.6° and C−D of 59.9° (*syn*). In the fjord regions, $H^8$ is in the process of passing the opposing $C^{8'}$ and $H^{8'}$ at a distance of 1.90 Å and 1.71 Å (34% and 28% overlap), respectively. Conformational inversion of the *anti*-folded conformations of dixanthylene may proceed in two steps via an intermediate, as outlined in Figure 19.

The $D_{2d}$ orthogonally twisted biradical [$\mathbf{t}_\perp$] is the transition state for rotation about the double bond. The biradical state has a relative energy of 16.4 kcal/mol; the length of the $C^9-C^{9'}$ bond is 1.460 Å. Obviously, there is no overcrowding in this conformation. For *E,Z* isomerization, the *anti*-folded global minimum conformation first has to be converted into a twisted conformation via a *syn*-folded conformation. An example is shown in Figure 20.

The $C_s$-symmetric pathway for the interconversion of the conformations **a** and **s** (synchronous double edge passage) does not have a bona fide transition state, but a second order saddle point ‖[**a-s**]‖$_{Cs}$. The relative energy of 16.9 kcal/mol renders it less favorable than [**a-s**].

The $C_2$-symmetric edge passage pathway from **a** to **t** passes through the second order saddle point ‖[**a-t**]‖ with a relative energy of 17.8 kcal/mol (**a** and **t** interconvert via the intermediate **s** and transition states [**a-s**] and [**s-t**], vide infra).

The planar conformation ‖[**p**]‖ has a relative energy of 140.3 kcal/mol and 9 negative Hessian matrix eigenvalues. It has no relevance to the dynamic stereochemistry. However, it illustrates the degree of overcrowding in a hypothetical planar conformation of dixanthylene.

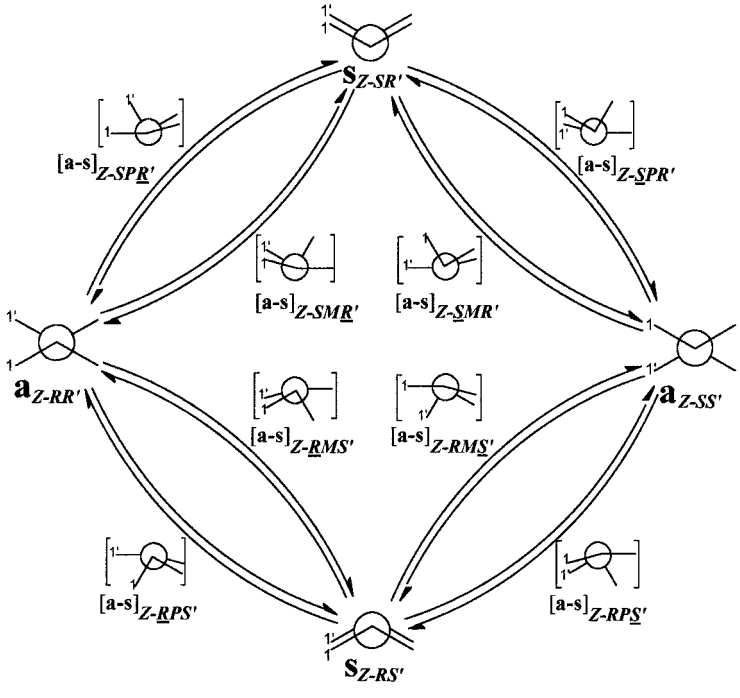


Figure 19. Network of pathways for the *anti*-folded, *syn*-folded conformational isomerization **a** ⇄ **s** via a folded/twisted transition state [**a-s**] of dixanthylene (**3**)

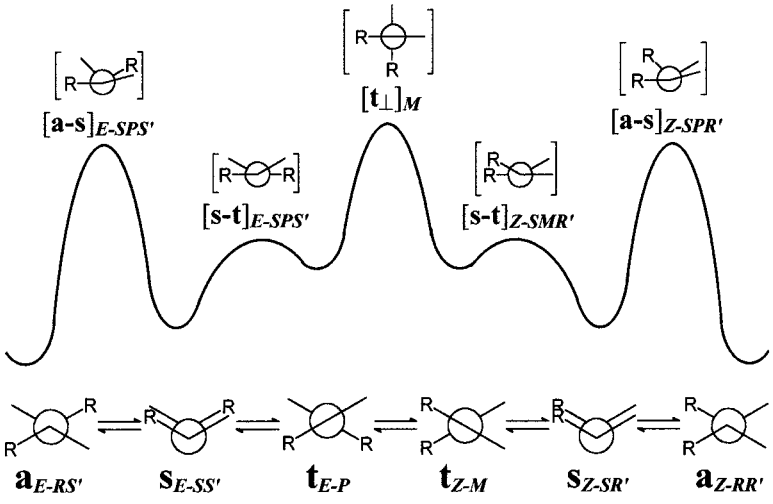


Figure 20. Example of a thermal *E,Z* isomerization pathway of a disubstituted dixanthylene, including a schematic energy profile

### 3.2 Dynamic Stereochemistry of Dixanthylene

The lowest dynamic barrier (9.5 kcal/mol) calculated for dixanthylene (**3**) corresponds to the interconversion of the *syn*-folded and twisted local minima **s** and **t** via [**s-t**] (bold arrows in Figure 21). The barrier for interconversion of the *anti*-folded global minimum **a** and the *syn*-folded conformation **s** is 15.9 kcal/mol. This conformational isomerization via the $C_1$-symmetric folded/twisted transition state [**a-s**] also facilitates the conformational inversion of the *anti*-folded conformation in two steps. The *E,Z* isomerization of **a** proceeds in 5 steps through intermediate *syn*-folded and twisted conformations, **s** and **t**. The highest transition state is the orthogonal biradical [$\mathbf{t}_\perp$] (16.3 kcal/mol).

Note that the PM3 dynamic mechanisms are different from those derived from the experimental results.[68] In the latter, a direct conversion of the *anti*-folded conformation to the twisted conformation was postulated. It is possible that a *syn*-folded intermediate may not have been detected because of its higher energy and very low equilibrium concentration. The experiments found essentially identical barriers for the *E,Z* isomerization, and conformational inversion [$\Delta G^{\ddagger}_{c}(E,Z)$ = 17.9 ± 0.3 kcal/mol and $\Delta G^{\ddagger}_{c}$(inv) = 17.7 ± 0.5 kcal/mol for 2,2′-diisopropyldixanthylene].[68]

## 4. Dithioxanthylene

Dithioxanthylene (**9**), a homomerous overcrowded bistricyclic aromatic ene with sulfur bridges, is a higher homologue of dixanthylene (**3**). It has an *anti*-folded global minimum conformation. However, **9** proved to be nonthermochromic in solution, contrary to dixanthylene (**3**).[45] A metastable *syn*-folded conformation was generated photochemically.[39,42] The 2D structure and atom labeling of dithioxanthylene are shown in Figure 22.

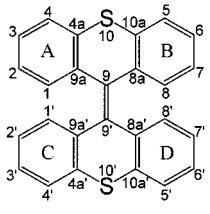


Figure 22. Structure and atom labeling in dithioxanthylene (**9**)

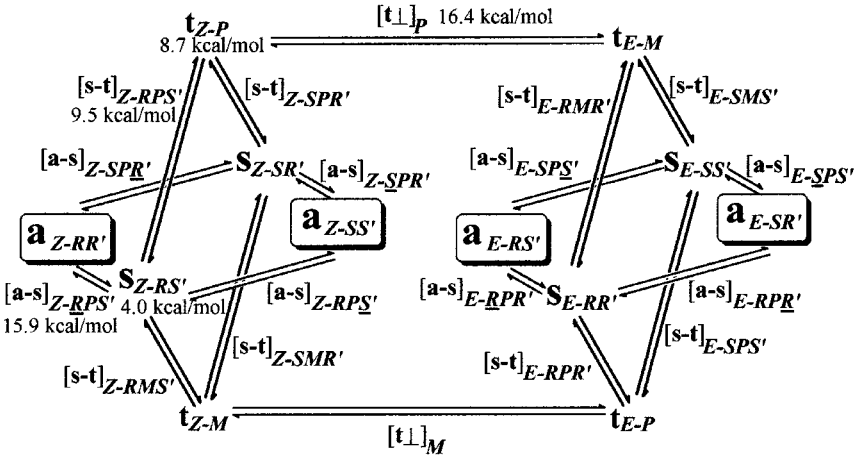


Figure 21. Scenario of the dynamic processes in dixanthylene (**3**)

### 4.1 Conformers and Transition States

For dithioxanthylene, 2 minima, 3 transition states, and 3 higher order saddle points were identified. The results are summarized in Table 7. 3D projections of the minima and transition states are shown in Figure 23 and Figure 24, respectively.

The global minimum conformation of dithioxanthylene is the $C_{2h}$-symmetric, *anti*-folded conformation **a**, with A−B = 46.8°. In the fjord regions, only the nonbonding distance C···C (3.13 Å) corresponds to overcrowding (9% overlap).

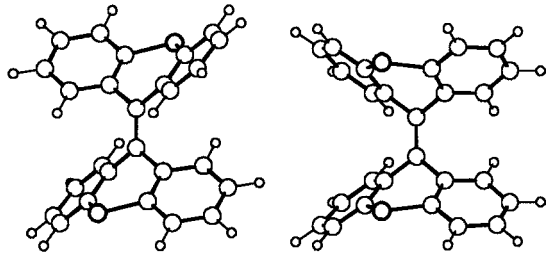

Figure 23. 3D projections of the *anti*-folded global minimum conformation **a** (left) and the *syn*-folded local minimum conformation **s** (right) of dithioxanthylene (**9**)

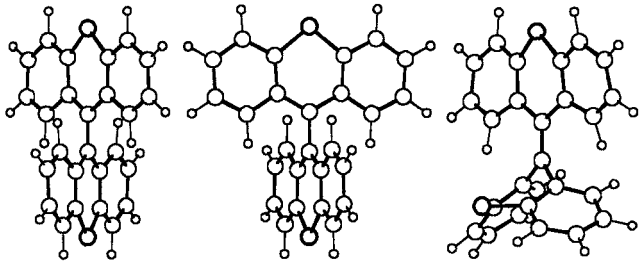

Figure 24. 3D projections of the transition states [**t**] (left), [$\mathbf{t}_\perp$] (center), and [**a-s**] (right) of dithioxanthylene (**9**)

The $C_{2v}$-symmetric, *syn*-folded conformation **s** is a local minimum. It is 3.3 kcal/mol higher in energy than **a** and considerably more folded, with A−B = 50.4°. The central double bond is not twisted but highly *syn*-pyramidalized, with $\chi(C^9)$ = 10.7°. The fjord-region hydrogen atoms are subject to severe overcrowding: H···H = 1.76 Å (23% overlap).

The $D_2$-symmetric, twisted conformation [**t**] is the transition state for inversion of the *syn*-folded conformation (Figure 25) with a relative energy of 20.1 kcal/mol. The central double bond $C^9{=}C^{9'}$ is twisted by 55.9° and is 0.05 Å longer than in **a**. The nonbonding distance C···C = 3.01 Å corresponds to overcrowding (12% overlap).

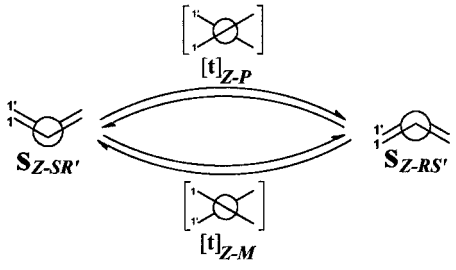


Figure 25. Scheme of the dynamic mechanism for inversion of the *syn*-folded conformation **s** via the twisted transition state [**t**] of dithioxanthylene (**9**)

The $D_{2d}$-symmetric, orthogonally twisted biradical [$\mathbf{t}_\perp$] is a transition state. Its conformational energy is 20.7 kcal/mol, only 0.5 kcal/mol higher than **t**. The central $C^9{-}C^{9'}$ bond is 1.477 Å. There is no intramolecular overcrowding in this conformation. The transition vector of [$\mathbf{t}_\perp$] is of symmetry species $B_1$ and leads to **t**-$D_2$ type structures. However, no local minimum energy conformation with $D_2$ symmetry was found for dithioxanthylene. The conformation [**t**] is a transition state. Thus, the pathways bifurcate[125,126] at the valley ridge inflection point (VRI)[127] between [$\mathbf{t}_\perp$] and [**t**] and lead to *syn*-folded conformations. The mechanism is outlined in Figure 26.

Table 7. Conformations of dithioxanthylene (**9**) calculated by PM3

| Conformation | | | [a] | PM3 $\Delta H_f°$ [kcal/mol] | $\Delta\Delta H_f°$ [kcal/mol] | ω[b] [°] | Folding A−B [°] | Bond $C^9{=}C^{9'}$ | $\chi(C^9)$ $\chi(C^{9'})$ | $C^1{\cdots}C^{1'}$ $C^8{\cdots}C^{8'}$ | $C^1{\cdots}H^{1'}$ $C^8{\cdots}H^{8'}$ | $H^1{\cdots}H^{1'}$ $H^8{\cdots}H^{8'}$ |
|---|---|---|---|---|---|---|---|---|---|---|---|---|
| **a** | *anti*-folded | **a**-$C_{2h}$ (y) | Min | 145.2 | 0.0 | 0.0 | 46.8 | 1.353 | −2.9 | 3.13 | 3.12 | 3.47 |
| **s** | *syn*-folded | **s**-$C_{2v}$ (x) | Min | 148.5 | 3.3 | 0.0 | 50.4 | 1.352 | 10.7 | 3.01 | 2.55 | 1.76 |
| [**t**] | twisted | **t**-$D_2$ | TS | 165.3 | 20.1 | 55.9 | 7.1 | 1.404 | 0.0 | 3.01 | 2.75 | 2.91 |
| [$\mathbf{t}_\perp$] | | $\mathbf{t}_\perp$-$D_{2d}$ | TS | 165.8 | 20.7 | 90.0 | 0.0 | 1.477 | 0.0 | 3.73 | 3.45 | 3.51 |
| [**a-s**] | | **ft**-$C_1$ | TS | 169.5 | 24.3 | 12.2 | 20.2 | 1.369 | 2.3 | 3.06 | 3.29 | 2.98 |
| | | | | | | | 68.4[c] | | 9.5 | 2.87 | 2.81 | 1.76 |
| | | | | | | | | | | | 2.41[c] | |
| | | | | | | | | | | | 1.84[c] | |
| ‖[**a-s**]‖$_{Cs}$ | | **f**-$C_s$ (xz) | 2 | 171.1 | 25.9 | 0.0 | 5.1 | 1.368 | 2.3 | 2.99 | 3.14 | 2.35 |
| | | | | | | | 72.5[c] | | 12.2 | | 1.97[c] | |
| ‖[**a-t**]‖ | | **ta**-$C_{2h}$ (y) | 2 | 175.4 | 30.2 | 58.1 | 30.3 | 1.397 | −7.3 | 3.75 | 4.00 | 4.39 |
| | | | | | | | | | | 3.36 | 2.46 | 1.48 |
| ‖[**p**]‖ | planar | **p**-$D_{2h}$ | 9 | 363.1 | 217.9 | 0.0 | 0.0 | 1.464 | 0.0 | 2.85 | 1.92 | 0.90 |

[a] Minimum (Min), transition state (TS), or number of imaginary frequencies of a higher order saddle point. − [b] Pure twist of central ethylene group. − [c] Refers to the second moiety.

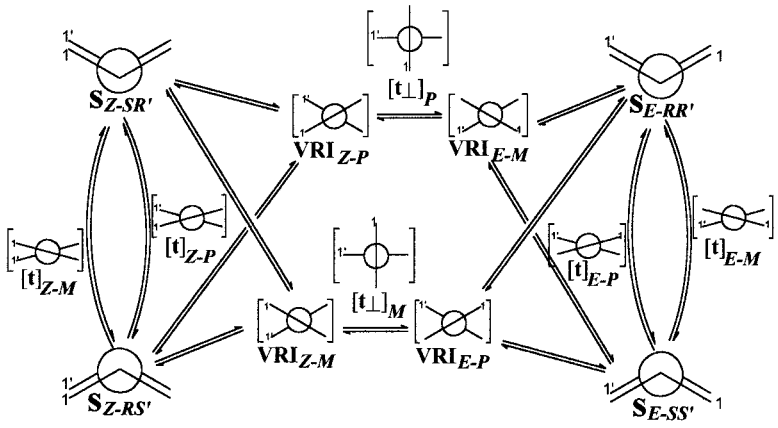


Figure 26. Thermal *E,Z* isomerization mechanism of the *syn*-folded conformations **s** in dithioxanthylene (**9**) via the orthogonally twisted transitions state [$\mathbf{t}_\perp$] and the Valley-Ridge inflection points VRI with $D_2$ symmetry, where the pathways bifurcate; the transition states [**t**] for inversion of the *syn*-folded conformations **s** are also included in the scheme

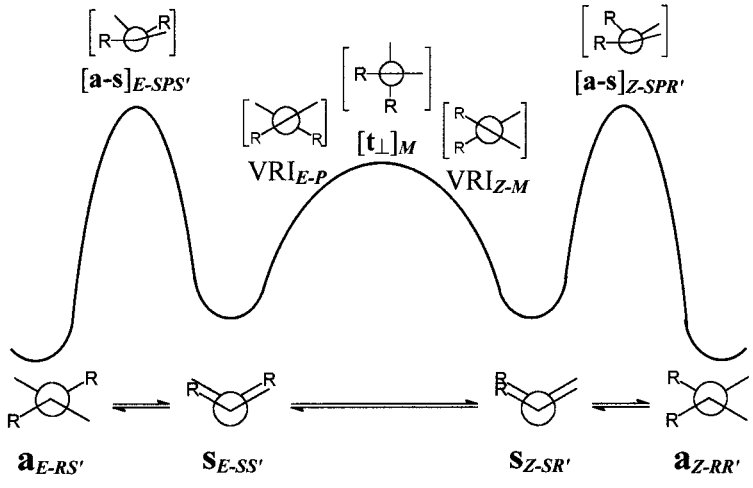


Figure 27. Example of a thermal *E,Z* isomerization pathway of a disubstituted dithioxanthylene (**9**), including a schematic energy profile; VRI is the Valley-Ridge inflection point at which the pathway bifurcates

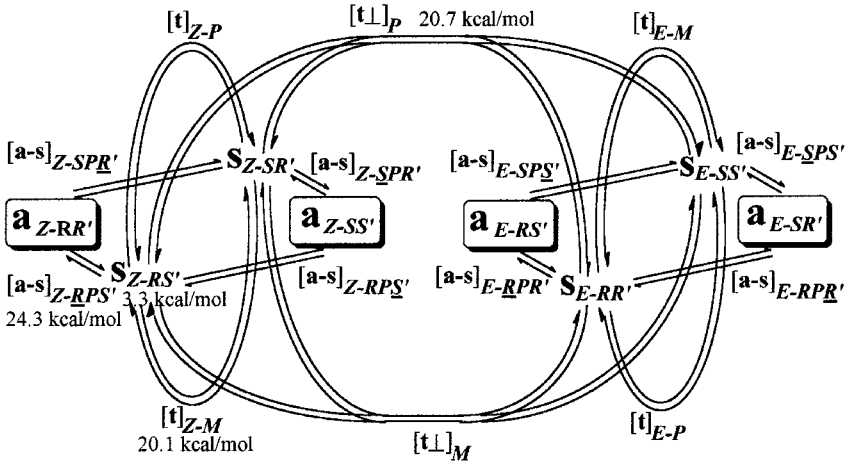


Figure 28. Scenario of the dynamic processes in dithioxanthylene (**9**)

The conformational isomerization of **a** to **s** may proceed via the transition state [**a-s**] (type **ft**-$C_1$), with a mechanism analogous to that for dixanthylene (Figure 19). The relative energy is 24.3 kcal/mol, the ethylenic twist ω = 12.2°, the A−B folding dihedral = 20.2°, and the C−D folding dihedral = 68.4°. Hydrogen atom $H^8$ is passing $H^{8'}$ and $C^{8'}$ at

distances of 1.76 Å and 1.84 Å (23% and 36% overlap), respectively. The [**a-s**] transition state facilitates the conformational inversion of **a** in a two-step process (Figure 19) and is the highest transition state for the *E,Z* isomerization of **a** by a three-step process. An example is shown in Figure 27.

The $C_s$-symmetric pathway from **a** to **s** (synchronous double edge passage) leads to the second-order saddle point ‖[**a-s**]‖$_{Cs}$ with a relative energy of 25.9 kcal/mol, and thus is less favorable than the above mechanism.

The $C_2$-symmetric pathway from **a** to [**t**] passes through the second order saddle point ‖[**a-t**]‖, with the high relative energy of 30.2 kcal/mol.

The $D_{2h}$-symmetric, planar structure ‖[**p**]‖ has nine imaginary vibrational frequencies. The very high relative energy of 217.9 kcal/mol and the highly distorted geometry illustrate the extreme level of overcrowding in a hypothetical planar dithioxanthylene.

### 4.2 Dynamic Stereochemistry of Dithioxanthylene

PM3 predicts high barriers for the dynamic stereochemistry of dithioxanthylene (**9**). The results are summarized in Figure 28. The conformational inversion of the *anti*-folded global minimum conformation **a** proceeds via the *syn*-folded intermediate **s** and the **ft**-$C_1$ type transition state [**a-s**] (24.3 kcal/mol barrier). The *E,Z* isomerizations proceed via the intermediates **s**, the orthogonal biradical transition state [$\mathbf{t}_\perp$] (20.6 kcal/mol), and bifurcating pathways. The highest transition state in this three-step process is [**a-s**]. Thus, in dithioxanthylene, [**a-s**] is the highest transition state common to both processes: the conformational inversion and the *E,Z* isomerization. The experimental barriers $\Delta G^{\ddagger}_{c}$(inv) and $\Delta G^{\ddagger}_{c}$(*E,Z*) are 27.4 kcal/mol for both processes.[103]

## 5. Bi-5*H*-dibenzo[*a,d*]cyclohepten-5-ylidene

Bi-5*H*-dibenzo[*a*,*d*]cyclohepten-5-ylidene (**11**), also known as tetrabenzoheptafulvalene, is a homomerous overcrowded bistricyclic aromatic ene with central 7-membered rings. The long bridges X = Y: CH=CH allow high degrees of folding. Both an *anti*-folded and a *syn*-folded conformation have been characterized by X-ray crystallography and by solution NMR spectroscopy.[72−76] In solution at high temperatures, the *syn*-folded conformation completely isomerizes to the *anti*-folded conformation.[76] The 2D structure and atom labeling used in this work are shown in Figure 29.

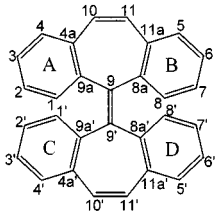


Figure 29. Structure of bi-5*H*-dibenzo[*a,d*]cyclohepten-5-ylidene (**11**) and atom labeling used in this work

### 5.1 Conformers and Transition States

The PM3 calculations located 2 minimum energy conformations, 2 transition states, and 4 higher order saddle points in the conformational space of bi-5*H*-dibenzo[*a*,*d*]cyclohepten-5-ylidene (**11**). The results are summarized in Table 8. The 3D projections of the minima and transition states are shown in Figure 30 and Figure 31, respectively.

The global minimum conformation of **11** is the *anti*-folded conformation **a**, with $C_{2h}$ symmetry. The folding dihedral A−B is 61.6°. Surprisingly, this conformation is not overcrowded in the fjord regions.

The second (local) minimum conformation is the *syn*-folded conformation **s**, with $C_{2v}$ symmetry and a relative energy of 0.5 kcal/mol. The folding dihedral A−B is 64.8° higher than in **a**. However, this conformation is overcrowded, with H···H = 1.81 Å (21% overlap).

The conformations **a** and **s** interconvert via the transition state [**a-s**] (type **ft**-$C_1$), with a relative energy of 37.6 kcal/mol. The mechanism is analogous to that of dixanthylene (Figure 19) and also allows conformational in-

Table 8. Conformations of bi-5*H*-dibenzo[*a,d*]cyclohepten-5-ylidene (**11**) calculated by PM3

| Conformation | | | [a] | PM3 $\Delta H_f°$ [kcal/mol] | $\Delta\Delta H_f°$ [kcal/mol] | ω[b] [°] | Folding A−B [°] | Bond $C^9=C^{9'}$ | $\chi(C^9)$ $\chi(C^{9'})$ | $C^1\cdots C^{1'}$ $C^8\cdots C^{8'}$ | $C^1\cdots H^{1'}$ $C^8\cdots H^{8'}$ | $H^1\cdots H^{1'}$ $H^8\cdots H^{8'}$ |
|---|---|---|---|---|---|---|---|---|---|---|---|---|
| **a** | *anti*-folded | **a**-$C_{2h}$ (y) | Min | 155.4 | 0.0 | 0.0 | 61.6 | 1.347 | −0.1 | 3.66 | 3.82 | 4.23 |
| **s** | *syn*-folded | **s**-$C_{2v}$ (x) | Min | 155.9 | 0.5 | 0.0 | 64.8 | 1.347 | 2.1 | 3.09 | 2.60 | 1.81 |
| [**a-s**] | | **ft**-$C_1$ | TS | 193.0 | 37.6 | 10.5 | 57.2 | 1.369 | 0.5 | 3.22 | 3.53 | 3.71 |
| | | | | | | | 78.7[c] | | 4.0 | 2.89 | 2.84<br>3.10[c] | 1.78 |
| | | | | | | | | | | | 2.04[c] | |
| [**ft**$_\perp$] | | **ts**-$C_2$ (x) | TS | 194.7 | 39.3 | 91.4 | 59.2 | 1.442 | 6.4 | 4.52 | 4.79<br>3.83 | 4.22 |
| ‖[**a-s**]‖$_{Cs}$ | | **f**-$C_s$ (xz) | 2 | 197.2 | 41.8 | 0.0 | 27.6 | 1.372 | −7.1 | 3.03 | 3.23 | 2.84 |
| | | | | | | | 87.4[c] | | 3.7 | | 2.29[c] | |
| ‖[**t**$_\perp$]‖ | | **t**$_\perp$-$D_{2d}$ | 2 | 203.7 | 48.3 | 90.0 | 0.0 | 1.499 | 0.0 | 3.54 | 3.30 | 3.40 |
| ‖[**t**]‖ | twisted | **t**-$D_2$ | 2 | 205.9 | 50.5 | 58.0 | 26.9 | 1.423 | 0.0 | 3.08 | 3.10 | 3.43 |
| ‖[**p**]‖ | planar | **p**-$D_{2h}$ | 13 | 519.3 | 363.9 | 0.0 | 0.0 | 1.509 | 0.0 | 2.89 | 1.87 | 0.85 |

[a] Minimum (Min), transition state (TS), or number of imaginary frequencies of a higher order saddle point. − [b] Pure twist of central ethylene group. − [c] Refers to the second moiety.

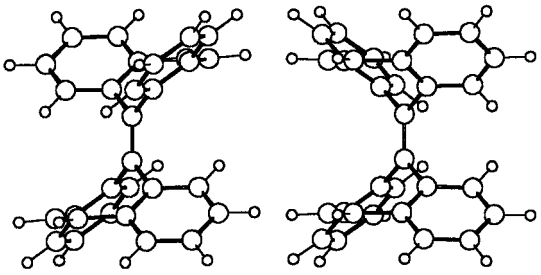

Figure 30. 3D projections of the *anti*-folded global minimum conformation **a** (left), and the *syn*-folded local minimum conformation **s** (right) of bi-5*H*-dibenzo[*a*,*d*]cyclohepten-5-ylidene (**11**)

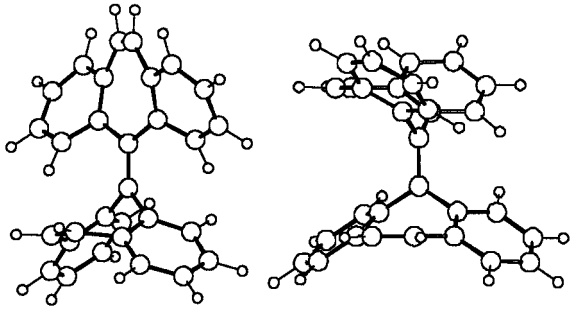

Figure 31. 3D projections of the transition states [**a-s**] (left) and [**ft**$_\perp$] (right) of bi-5*H*-dibenzo[*a*,*d*]cyclohepten-5-ylidene (**11**)

version of **a**. Both tricyclic moieties are highly nonplanar: A−B = 57.2° and C−D = 78.7°. Hydrogen atom $H^8$ is in the process of passing $H^{8'}$ and $C^{8'}$ at short distances: 1.78 Å and 2.04 Å (23% and 29% overlap), respectively. The high barrier, as compared to dithioxanthylene (**9**) and dixanthylene (**3**), may also reflect the lower degree of intramolecular overcrowding of the *anti*-folded and *syn*-folded conformations of **11**.

The $C_2$-symmetric biradical transition state [**ft**$_\perp$] has an almost orthogonally twisted central $C^9-C^{9'}$ bond, with ω = 88.6°. The relative energy is 39.3 kcal/mol. Each tricyclic moiety is folded by A−B = 59.2°. The nonbonding distances $C^1\cdots H^{8'}$ = 2.56 Å and $H^1\cdots H^{8'}$ = 1.79 Å correspond to overcrowding (14% and 22% overlap). The tricyclic moieties remain folded during the rotation about the central double bond. Thus, simultaneously with the *E,Z* isomerization, an *anti*-folded conformation is converted into a *syn*-folded conformation and vice versa, as shown in Figure 32.

The symmetry-constrained $C_s$ pathway (synchronous double edge passage) from **a** to **s** crosses the second-order saddle point ‖[**a-s**]‖$_{Cs}$, with a relative energy of 41.8 kcal/mol.

The $D_{2d}$-symmetric, orthogonally twisted biradical ‖[**t**$_\perp$]‖ is a second order saddle point, with a relative energy of 48.3 kcal/mol.

The $D_2$-symmetric conformation ‖[**t**]‖ is a second order saddle point, with a relative energy of 50.5 kcal/mol. This explains why bi-5*H*-dibenzo[*a*,*d*]cyclohepten-5-ylidene (**11**) is not thermochromic.

The $D_{2h}$-symmetric, planar conformation ‖[**p**]‖ has a very high energy of 364 kcal/mol and a highly distorted geometry due to the extreme intramolecular overcrowding. There are 13 imaginary frequencies.

### 5.2 Dynamic Stereochemistry of Bi-5*H*-dibenzo[*a*,*d*]-cyclohepten-5-ylidene

Figure 33 summarizes the dynamic stereochemistry of bi-5*H*-dibenzo[*a*,*d*]cyclohepten-5-ylidene (**11**). PM3 predicts the local minimum *syn*-folded conformation **s** to be only 0.5 kcal/mol higher than the global minimum *anti*-folded conformation **a**. The isomerization of the *anti*-folded and *syn*-folded conformations via the **ft**-$C_1$ type transition state [**a-s**] (37.6 kcal/mol), which also facilitates the inversion of **a** (and **s**), is similar to the inversion mechanisms found for

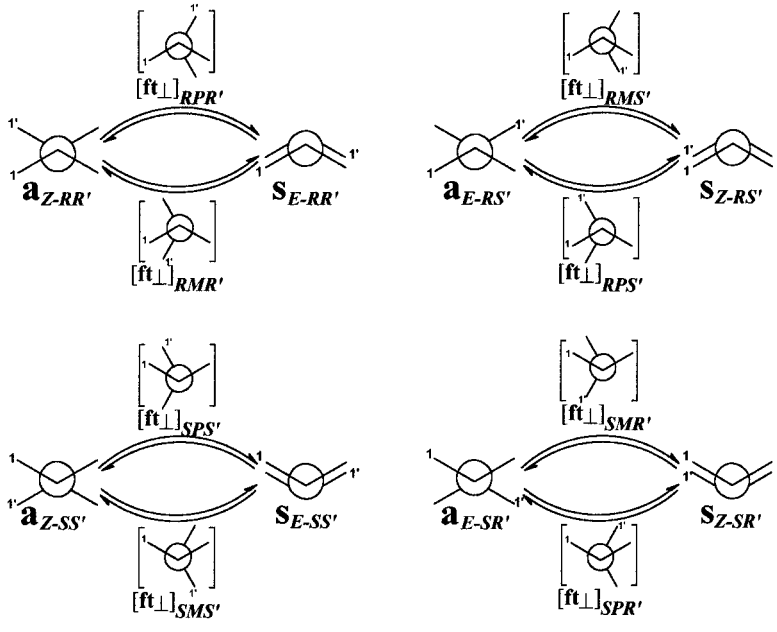


Figure 32. Pathways for the *E,Z* isomerization with simultaneous *anti,syn* isomerization via the transition state [**ft**$_\perp$] in bi-5*H*-dibenzo[*a,d*]-cyclohepten-5-ylidene (**11**)

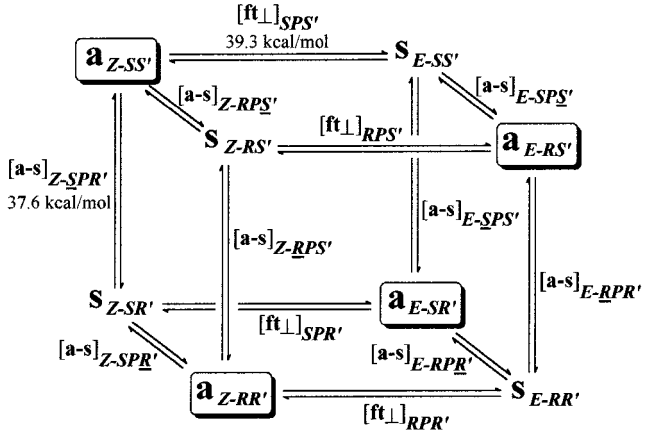


Figure 33. Scenario of the dynamic processes in bi-5*H*-dibenzo[*a,d*]cyclohepten-5-ylidene (**11**)

dixanthylene (**3**) and dithioxanthylene (**9**). The *E,Z* isomerization of **11** involves a simultaneous *anti,syn* isomerization, because the tricyclic moieties remain folded in the orthogonally twisted transition state [**ft**$_\perp$] (39.7 kcal/mol).

For **11**, the experimental barrier $\Delta G^{\ddagger}$ for the process **s** → **a** is 36.4 kcal/mol.[73] Adding the PM3-calculated relative energy of **s** − 0.5 kcal/mol − one arrives at 36.9 kcal/mol, which compares very well with the PM3-calculated energy of the [**a-s**] transition state: 37.6 kcal/mol. However, the complete conversion of **s** to **a** observed in the experiment[76] is not consistent with the calculated relative energy of 0.5 kcal/mol.

In cases where a pure stereoisomer of a disubstituted *syn*-folded **11** (**s**$_{E\text{-}RR'}$) can be isolated, it should be possible to determine both barriers in a kinetic experiment. The products **a**$_{E\text{-}RS'}$ and **a**$_{E\text{-}SR'}$ should be formed at a different rate from **a**$_{Z\text{-}RR'}$.

## 6. Conclusions

The PM3 calculations of the minima and transition states of overcrowded bistricyclic aromatic enes give a detailed picture of the dynamic stereochemistry and the energetic and geometric effects involved in the conformational isomerizations of bistricyclic enes.

The conformational energies of the twisted conformation, the *syn*-folded conformation, and of the most important transition states are summarized in Table 9. For comparison, experimental values are given in parenthesis.

The PM3-calculated and experimentally determined barriers of the thermal *E,Z* isomerization processes and conformational inversion processes agree within 1−3 kcal/mol. Only the energy of the highest transition state for enantiomerization of bifluorenylidene (**2**) − [**ta-at**] − is underestimated (4.9 versus 10.5 kcal/mol[67]). Formally, the computed energy barriers in Table 9 are enthalpies ($\Delta H^{\ddagger}$), while the experimental barriers are free energies ($\Delta G^{\ddagger}_{c}$). However, in these monomolecular conformational isomerizations, the contributions of entropy are small.[50,102] New mechanisms are proposed for the conformational inversion processes of dixanthylene (**3**), dithioxanthylene (**9**), and bi-5*H*-dibenzo[*a,d*]cyclohepten-5-ylidene (**11**): in two steps via folded/twisted (type **ft**-$C_1$) transition states [**a-s**] and the *syn*-folded intermediate **s**. The mechanisms for *E,Z* isomerization of **3** and **9** include **a** ⇄ **s** isomerizations as initial and final steps. In **9**, [**a-s**] is the highest transition state for *E,Z* isomerization, while in **3** the orthogonally twisted biradical transition state [**t**$_\perp$] is calculated to be slightly higher. For **11**, a unique mechanism with simultaneous *E,Z* and *syn,anti* isomerization was found. It is interesting to note that low-symmetry mechanisms, bypassing highly strained conformations, are preferred over the "high symmetry", or "least motion", mechanisms that might be expected intuitively.

Hopefully, the elucidation of the dynamic stereochemistry of the parent homomerous bistricyclic enes as a function of their molecular structure will contribute towards the development of the molecular architecture of new polycyclic aromatics and molecular devices with novel and interesting properties.

## Acknowledgments

The present Microreview is a fruition of a collaboration conceived in 1986 during Israel Agranat's first visit to Germany at the invitation of Professor K. Hafner and to the University of Stuttgart at the invitation of Professor Franz Effenberger. We thank the late Dr. Yitzhak Tapuhi, Dr. Shmuel Cohen, Dr. Michal Rachel Suissa, Dr. Amalia Levy and Mr. Sergey Pogodin for their significant contributions to the chemistry of overcrowded bistricyclic aromatic enes. P. U. B. thanks the Minerva Foundation for a Minerva Fellowship and the Deutscher Akademischer Austauschdienst for a Kurzstipendium.

Table 9. Energies of the twisted and *syn*-folded conformations and of the transition states for enantiomerization, conformational inversion, and *E,Z* isomerization, relative to the global minimum (*anti*-folded) conformations of **2**, **3**, **9**, and **11** [kcal/mol]

| | Twisted conformation[a] | | *syn*-Folded conformation | | Enantiomerization or inversion barrier[a] | | *E,Z* Isomerization barrier[a] | |
|---|---|---|---|---|---|---|---|---|
| **2** | **t** | 0.2[b] | [**s**] | 8.4[b] | [**ta-at**] | 4.9[b] (10.5)[67] | [**t**$_\perp$] | 25.2[b] (25.0)[67] |
| **3** | **t** | 8.7 (4.9,[45] 5.6)[46] | **s** | 4.0 | [**a-s**] | 15.9 (17.7)[68] | [**t**$_\perp$] | 16.4 (17.9)[68] |
| **9** | [**t**] | 20.1 | **s** | 3.3 | [**a-s**] | 24.3 (27.4)[103] | [**a-s**] | 24.3 (27.4)[103] |
| **11** | ‖[**t**]‖[c] | 50.5 | **s** | 0.5 | [**a-s**] | 37.6 (36.9)[d] | [**ft**$_\perp$] | 39.3 |

[a] Experimental values are given in parenthesis where available. − [b] Relative to the global minimum **ta**. − [c] Second order saddle point. − [d] Composed from $\Delta E_{rel}$(**s**) = 0.5 kcal/mol (PM3) and the exptl. barrier for **s** → **a** of 36.4 kcal/mol.[73]

[1] G. Shoham, S. Cohen, R. M. Suissa, I. Agranat, in *Molecular Structure: Chemical Reactivity and Biological Activity* (Eds.: J. J. Stezowski, J.-L. Huang, M.-C. Shao), IUCr Crystallographic Symposia 2, Oxford University Press, Oxford, **1988**, pp. 290−312.

[2] P. U. Biedermann, J. J. Stezowski, I. Agranat, in: *Advances in Theoretically Interesting Molecules*, vol. 4 (Ed.: R. P. Thummel), JAI Press, Stamford, Connecticut **1998**, pp. 245−322

[3] C. de la Harpe, W. A. Van Dorp, *Ber. Dtsch. Chem. Ges.* **1875**, *8*, 1048−1050.

[4] G. Gurgenjanz, S. v. Konstanecki, *Ber. Dtsch. Chem. Ges.* **1895**, *28*, 2310−2311.

[5] H. Meyer, *Monatsh. Chem.* **1909**, *30*, 165−177.

[6] H. Meyer, *Ber. Dtsch. Chem. Ges.* **1909**, *42*, 143−145.

[7] P. U. Biedermann, A. Levy, J. J. Stezowski, I. Agranat, *Chirality* **1995**, *7*, 199−205.

[8] R. L. Avoyan, Y. T. Struchkov, V. G. Dashevskii, *J. Struct. Chem. (USSR)* **1966**, *7*, 283−320.

[9] J. Sandström, *Top. Stereochem.* **1983**, *14*, 83−181.

[10] W. Luef, R. Keese, *Top. Stereochem.* **1991**, *20*, 231−318.

[11] J. Sandström, in: *The chemistry of double-bonded functional groups*, *Supplement A3*, (Ed.: S. Patai), Wiley, New York, **1997**, pp. 1253−1280.

[12] B. L. Feringa, A. M. Schoevaars, W. F. Jager, B. de Lange, N. P. M. Huck, *Enantiomer* **1996**, *1*, 325−335.

[13] W. F. Jager, B. de Lange, A. M. Schoevaars, F. van Bolhuis, B. L. Feringa, *Tetrahedron: Asymmetry* **1993**, *4*, 1481−1497.

[14] B. L. Feringa, W. F. Jager, B. de Lange, *Tetrahedron* **1993,** *49*, 8267−8310.

[15] B. de Lange, W. F. Jager, B. L. Feringa, *Mol. Cryst. Liq. Cryst.* **1992**, *217*, 129−132.

[16] W. F. Jager, B. de Lange, B. L. Feringa, *Mol. Cryst. Liq. Cryst.* **1992**, *217*, 133−138.

[17] J. J. Stezowski, T. Hildenbrand, M. R. Suissa, I. Agranat, *Struct. Chem.* **1990**, *1*, 123−126.

[18] S. Hagen, U. Nuechter, M. Nuechter, G. Zimmermann, *Tetrahedron Lett.* **1994**, *35*, 7013−7014.

[19] S. Hagen, U. Nuechter, M. Nuechter, G. Zimmermann, *Polycycl. Aromat. Compd.* **1995**, *4*, 209−217.

[20] P. U. Biedermann, T.-Y. Luh, D. T.-C.Weng, C.-H. Kuo, J. J. Stezowski, I. Agranat, *Polycycl. Aromat. Compd.* **1996**, *8*, 167−175.

[21] S. Pogodin, P. U. Biedermann, I. Agranat, in *Recent Advances in the Chemistry of Fullerenes and Related Materials*, vol. 6 (Eds.: K. M. Kadish, R. S. Ruoff), The Electrochemical Society, Pennington, NJ, **1998**, pp. 1110−1116.

[22] P. W. Rabideau, A. Sygula, *Acc. Chem. Res.* **1996**, *29*, 235−242.

[23] L. T. Scott, *Pure Appl. Chem.* **1996**, *68*, 291.

[24] S. Pogodin, P. U. Biedermann, I. Agranat, *J. Org. Chem.* **1997**, *62*, 2285−2287.

[25] G. Mehta, H. S. P. Rao, in *Advances in Strain in Organic Chemistry* (Ed.: B. Halton), JAI Press, London, **1997**, vol. 6, pp 139−187.

[26] G. Mehta, H. S. P. Rao, *Tetrahedron* **1998**, *54*, 13325−13370.

[27] P. W. Rabideau, A. Sygula, in *Advances in Theoretically Interesting Molecules* (Ed.: R. P. Thummel), JAI Press, Greenwich, CT, **1995**, vol. 3, pp. 1−30.

[28] H. Decker,W. Petch, *J. Pract. Chem.* **1935**, *143*, 211.

[29] A. Albert, *The Acridines: Their Preparation, Physical Properties, Chemical and Biological Properties and Uses*, 2nd ed., Edward Arnold, London, **1966**, pp. 392−393 and 540.

[30] T. J. Nagem, V. L. Alves, *Fitoterapia* **1995**,*66*, 278; T. Nagem, M. A. Ferriera, *Fitoterapia* **1993**, *64*, 382−383.

[31] K. Linde, G. Ramirez, C. D. Mulrow, A. Pauls, W. Weidenhammer, D. Melchart, *Br. Med. J.* **1996**, *313*, 253−258.

[32] M. Philipp, R. Kohnen, K.-O. Hiller, *Br. Med. J.* **1999**, *319*, 1534−1539.

[33] D. Lavie, D. Freeman, H. Bock, J. Fleischer, K. van Kranenburg, Y. Ittah, Y. Mazur, G. Lavie, L. Liebes, D. Meruelo, in *Trends in Medicinal Chemistry '90. Proceedings of the XIth International Symposium on Medicinal Chemistry*, Jerusalem, Israel, **1990** (Eds.: S. Sarel, R. Mechoulam, I. Agranat), International Union of Pure and Applied Chemistry, Blackwell Scientific Publications, Oxford **1992**, pp. 321−327.

[34] G. Lavie, F. Valentine, B. Levin, Y. Mazur, G. Gallo, D. Lavie, D. Weiner, D. Meruelo, *Proc. Natl. Acad. Sci.* **1989**, *86*, 5963−5967.

[35] E. D. Bergmann, *Prog. Org. Chem.* **1955**, *3*, 81−171.

[36] J. H. Day, *Chem. Rev.* **1963**, *63*, 65−80.

[37] G. Kortüm, *Ber. Bunsenges. Phys. Chem.* **1974**, *78*, 391−403.

[38] Y. Tapuhi, O. Kalisky, I. Agranat, *J. Org. Chem.* **1979**, *44*, 1949−1952.

[39] E. Fischer, *Rev. Chem. Intermed.* **1984**, *5*, 393−422.

[40] K. A. Muszkat, in *The Chemistry of Quinonoid Compounds*, vol. II, (Eds.: S. Patai, Z. Rappoport), Wiley, Chichester, **1988**, p. 203−224.

[41] R. Korenstein, K. A. Muszkat, G. Seger, *J. Chem. Soc., Perkin Trans. 2* **1976**, 1536−1540.

[42] R. Korenstein, K. A. Muszkat, E. Fischer, *J. Photochem.* **1976**, *5*, 345−353.

[43] D. L. Franselow, H. G. Drickamer, *J. Chem. Phys.* **1974**, *61*, 4567−4574.

[44] W. T. Grubb, G. B. Kistiakowsky, *J. Am. Chem. Soc.* **1950**, *72*, 419−424.

[45] W. Theilacker, G. Kortüm, G. Friedheim, *Chem. Ber.* **1950**, *83*, 508−519.

[46] Y. Hirschberg, E. Fischer, *J. Chem. Soc.* **1953**, 629−636.

[47] J. F. D. Mills, S. C. Nyburg, *J. Chem. Soc.* **1963**, 308−321.

[48] J. F. D. Mills, S. C. Nyburg, *J. Chem. Soc.* **1963**, 927−935.

[49] E. Ahlberg, O. Hammerich, V. D. Parker, *J. Am. Chem. Soc.* **1981**, *103*, 844−849.

[50] O. Hammerich, V. D. Parker, *Acta Chem. Scand.* **1981**, *35B*, 395−402.

[51] P. Neta, D. H. Evans, *J. Am. Chem. Soc.* **1981**, *103*, 7041−7045.

[52] B. A. Olsen, D. H. Evans, *J. Am. Chem. Soc.* **1981**, *103*, 839−843.

[53] B. A. Olsen, D. H. Evans, I. Agranat, *J. Electroanal. Chem.* **1982**, *136*, 139−148.

[54] D. H. Evans, R. W. Busch, *J. Am. Chem. Soc.* **1982**, *104*, 5057−5062.

[55] D. H. Evans, N. Xie, *J. Electroanal. Chem.* **1982**, *133*, 367−373.

[56] D. H. Evans, N. Xie, *J. Am. Chem. Soc.* **1983**, *105*, 315−320.

[57] D. H. Evans, A. Fitch, *J. Am. Chem. Soc.* **1984**, *106*, 3039−3041.

[58] T. Matsue, D. H. Evans, I. Agranat, *J. Electroanal. Chem.***1984**, *163*, 137−143.

[59] M. Jørgensen, K. Lerstrup, P. Frederiksen, T. Bjørnholm, P. Sommer-Larsen, K. Schaumburg, K. Brunfeldt, K. Bechgaard, *J. Org. Chem.* **1993**, *58*, 2785−2790.

[60] J. J. P. Stewart, *J. Comput. Chem.***1989**, *10*, 221−264.

[61] F. Bell, D. H. Waring, *J. Chem. Soc.* **1949**, 2689−2693.

[62] E. Harnik, F. H. Herbstein, G. M. J. Schmidt, *Nature* **1951**, *168*, 158−160.

[63] E. Bergmann, *J. Chem. Soc.* **1935**, 987−989.

[64] M. Rabinovitz, I. Agranat, E. D. Bergmann, *Tetrahedron Lett.* **1965**, *18*, 1265−1269.

[65] N. A. Bailey, S. E. Hull, *Acta Crystallogr., B* **1978**, *34*, 3289−3295.

[66] J.-S. Lee, S. C. Nyburg, *Acta Crystallogr., C* **1985**, *41*, 560−567.

[67] P. U. Biedermann, A. Levy, M. R. Suissa, J. J. Stezowski, I. Agranat, *Enantiomer* **1996**, *1*, 75−80.

[68] I. Agranat, Y. Tapuhi, *J. Am. Chem. Soc.* **1979**, *101*, 665−671.

[69] E. Harnik, G. M. J. Schmidt, *J. Chem. Soc.* **1954**, 3295−3302.

[70] P. A. Apgar, E. Wasserman, unpublished results, **1978** (quoted in ref.[1]).

[71] I. Agranat, Y. Tapuhi, *J. Am. Chem. Soc.* **1978**, *100*, 5604−5609.

[72] K. S. Dichmann, S. C. Nyburg, F. H. Pickard, J. A. Potworowski, *Acta Crystallogr., B* **1974**, *30*, 27−36.

[73] I. Agranat, M. R. Suissa, *Struct. Chem.* **1993**, *4*, 59−66.

[74] E. D. Bergmann, M. Rabinovitz, I. Agranat, *Chem. Commun.* **1968**, 334−335.

[75] A. Schönberg, U. Sodtke, K. Präfcke, *Tetrahedron Lett.* **1968**, 3253−3256.

[76] A. Schönberg, U. Sodtke, K. Präfcke, *Chem. Ber.* **1969**, *102*, 1453−1467.

[77] Y. Tapuhi, M. R. Suissa, S. Cohen, P. Ulrich Biedermann, A. Levy, I. Agranat, *J. Chem. Soc., Perkin Trans. 2* **2000**, 93−100.

[78] A. Z.-Q. Khan, J. Sandström, *J. Am. Chem. Soc.* **1988**, *110*, 4843−4844.
[79] A. Greenberg, J. F. Liebman, *Strained Organic Molecules*, Academic Press, New York, **1978**, p. 91.
[80] R. C. Haddon, *Chem. Phys. Lett.* **1986**, *125*, 231−234.
[81] R. C. Haddon, *J. Am. Chem. Soc.* **1987**, *109*, 1676−1685.
[82] W. T. Borden, *Chem. Rev.* **1989**, *89*, 1095−1109.
[83] R. C. Haddon, *J. Am. Chem. Soc.* **1990**, *112*, 3385−3389.
[84] T. P. Radhakrishnan, I. Agranat, *Struct. Chem.* **1991**, *2*, 107−115.
[85] A. P. Scott, I. Agranat, P. U. Biedermann, N. V. Riggs, L. Radom, *J. Org. Chem*. **1997**, *62*, 2026−2038.
[86] G. Helmchen, *Methods Org. Chem. (Houben-Weyl)*, **1995**, vol. E21a, p. 1−75.
[87] W. Klyne, V. Prelog, *Experientia* **1960**, *16*, 521−523.
[88] I. Agranat, Y. Tapuhi, J. Y. Lallemand, *Nouv. J. Chim.* **1979**, *3*, 59−61.
[89] R. S. Cahn, C. K. Ingold, *J. Chem. Soc.* **1951**, 612−622.
[90] R. Kuhn, H. Zahn, K. L. Scholler, *Justus Liebigs Ann. Chem.* **1953**, *582*, 196−217
[91] I. R. Gault, W. D. Ollis, I. O. Sutherland, *J. Chem. Soc., Chem. Commun.* **1970**, 269−271.
[92] I. O. Sutherland, *Annu. Rep. NMR Spectrosc.* **1971**, *4*, 71−235.
[93] I. Agranat, M. Rabinovitz, A. Weitzen-Dagan, I. Gosnay, *J. Chem. Soc., Chem. Commun.* **1972**, 732−733.
[94] I. Agranat, M. Rabinovitz, I. Gosnay, A. Weitzen-Dagan, *J. Am. Chem. Soc.* **1972**, *94*, 2889−2891.
[95] M. Rabinovitz, I. Agranat, A. Weitzen-Dagan, *Tetrahedron Lett.* **1974**, 1241−1244.
[96] I. Agranat,Y. Tapuhi, *J. Am. Chem. Soc.* **1976**, *98*, 615−616.
[97] I. Agranat,Y. Tapuhi, *Nouv. J. Chim.* **1977**, *1*, 361−362.
[98] I. Agranat,Y. Tapuhi, *J. Org. Chem.* **1979**, *44*, 1941−1948.
[99] J. Bindl, T. Burgemeister, J. Daub, *Chem. Ber.* **1985**, *118*, 4934−4945.
[100] X.-j. Wang, T.-Y. Luh, *J. Org. Chem.* **1989**, *54*, 263−265.
[101] Y. C. Yip, X.-j. Wang, D. K. P. Ng, T. C. W. Mak, P. Chiang,T.-Y. Luh, *J. Org. Chem. 55*, 1881−1889, **1990**.
[102] U. Grieser, K. Hafner, *Tetrahedron Lett.* **1994**, *35*, 7759−7762
[103] B. L. Feringa, W. F. Jager, B. de Lange, *Tetrahedron Lett.* **1992**, *33*, 2887−2890.
[104] B. L. Feringa, W. F. Jager, B. de Lange, *J. Chem. Soc., Chem. Commun.* **1993**, 288−290.
[105] E. M. Geertsema, A. Meetsma, B. L. Feringa, *Angew. Chem. Int. Ed.* **1999**, *38*, 2738−2741.
[106] M. Oki, *Applications of Dynamic NMR Spectroscopy to Organic Chemistry*, VCH, Deerfield Beach, FL, **1985**, pp. 108−111.
[107] E. L. Eliel, S. H. Wilen, L. N. Mander, *Stereochemistry of Organic Compounds*, Wiley, New York, **1994**, p. 546−548.
[108] S. Wawzonek, J. P. Henry, *J. Org. Chem.* **1953**, *18*, 1461−1465.
[109] W. J. Leigh, D. R. Arnold, *Can. J. Chem.* **1981**, *59*, 609−620.
[110] P. Sommer-Larsen, T. Bjørnholm, M. Jørgensen, K. Lerstrup, P. Frederiksen, K. Schaumburg, K. Brunfeldt, K. Bechgaard, S. Roth, J. Poplawski, H. Byrne, J. Anders, L. Eriksson, R. Wilbrandt, J. Ferderiksen, *Mol. Cryst. Liq. Cryst.* **1993**, *234*, 89−96.
[111] K. Schaumburg, J.-M. Lehn, V. Goulle, S. Roth, H. Byrne, S. Hagen, J. Poplawski, K. Brunfeldt, K. Bechgaard, T. Bjørnholm, P. Frederiksen, M. Jørgensen, K. Lerstrup, P. Sommer-Larsen, O. Goscinski, J.-L. Calais, L. Eriksson, *Proceedings of the CEC Workshop on Nanostructures Based upon Molecular Materials*, Tübingen, **1991** (Ed.: W. Göpel), VCH, Weinheim, **1992**, pp. 153−173.
[112] A. Levy, P. U. Biedermann, S. Cohen, I. Agranat, *J. Chem. Soc., Perkin Trans. 2* **2000**, 725−735.
[113] O. Kikuchi, K.-I. Matsushita, K. Morihashi, M. Nakayama, *Bull. Chem. Soc. Jpn.* **1986**, *59*, 3043−3046.
[114] O. Kikuchi, Y. Kawakami, *J. Mol. Struct. (Theochem)* **1986,** *137*, 365−372.
[115] S. Kammermeier, R. Herges, *Angew. Chem. Int. Ed. Engl.* **1996**, *35*, 417−419.
[116] A. Levy, P. U. Biedermann, I. Agranat, *Org. Lett.* **2000**, *2*, 1811−1814.
[117] J. J. P. Stewart, MOPAC 6.00, *QCPE* 455, **1990**.
[118] J. J. P. Stewart, *MOPAC Manual*, 6th ed., Frank J. Seiler Research Laboratory, United States Air Force Academy, Colorado Springs, **1990**.
[119] Keywords (see ref.[118]) PM3 PRECISE SYMMETRY EF GNORM=0.1 and a z-matrix, including dummy atoms, which reflects the symmetry. The orthogonally twisted conformations were calculated as biradicals, adding the keyword BIRADICAL.
[120] Keywords PM3 PRECISE SYMMETRY FORCE and the optimized z-matrix of the archive file. For the orthogonally twisted conformations, the keyword BIRADICAL was added and PRECISE was omitted.
[121] Keywords PM3 PRECISE SYMMETRY EF GNORM=0.1 for minima, and PM3 PRECISE SYMMETRY TS HESS=1 GNORM=0.1 for transition states. In cases where the transition state optimizations did not converge, the keywords RECALC=1 and DMAX=0.02 were added in a second and third try.
[122] For the IRC calculations, the dummy atoms and symmetry constraints were removed from the z-matrix in a MOPAC6 calculation with the keywords PM3 1SCF XYZ (symmetry constraints cannot be used in MOPAC6 intrinsic reaction coordinate calculations). Second derivatives were recalculated for this new z-matrix, using the keywords PM3 PRECISE FORCE ISOTOPE. Starting from these results, two IRC calculations for each transition state were run to follow the normal mode with imaginary frequency in both directions. The keywords were: PM3 PRECISE IRC=1 GNORM=.01 LARGE LET X-PRIORITY=5 NOINTER RESTART ISOTOPE. In cases where the calculation ran out of time, it was restarted using the Keywords PM3 PRECISE IRC GNORM=.01 LARGE LET X-PRIORITY=5 NOINTER RESTART ISOTOPE.
[123] Y. V. Zefirov, *Crystallogr. Rep.* **1997**, *42*, 111−116.
[124] J. N. Murrell, K. J. Laidler, *Trans. Faraday Soc.* **1968**, *64*, 371−377.
[125] D. K. Hoffman, R. S. Nord, K. Ruedenberg, *Theor. Chim. Acta* **1986**, *69*, 265−279.
[126] L. J. Schaad, J. Hu, *J. Am. Chem. Soc.* **1998**, *120*, 1571−1580.
[127] P. Valtazanos, K. Ruedenberg, *Theor. Chim. Acta* **1986**, *69*, 281−307.

Received February 17, 2000
[O00080]